



Hamburg University of Applied Sciences

Faculty of Life Sciences

Investigation of tryptophan fluorescence as a tool for the analysis of oligomerisation and folding of antimicrobial peptides and lysozyme

Bachelor-Thesis

Biotechnology

submitted by

Maya Kamila, Dibyana



Hamburg, 22.09.23

First reviewer : Prof. Dr. Jörg Andrä (HAW Hamburg)
Second reviewer : Prof. Dr. Christian Kaiser (HAW Hamburg)

The thesis was supervised and prepared in the laboratory of HAW Hamburg

Abstract

Despite ongoing medical advancements and widespread use of antibiotics, bacteria continue to cause serious infections all over the world, necessitating the need for alternatives. Antimicrobial peptides (AMPs) have raised interest for a new development of drugs and one of the main advantages of this class of molecules is their activity against wide range of microorganisms including bacteria, fungi, viruses and even tumor cells. By focusing on recent insights into the folding and oligomerization of AMPs can yield information into their mechanism of action such as their interactions with bacterial membrane.

Tryptophan fluorescence measurements is used to investigate the oligomerisation of AMPs since the structure of AMPs that were analyzed on this paper have tryptophan residues which are classified as hydrophobic amino acid. The fluorescence of tryptophan exhibits an increase in intensity when the hydrophobicity of the surrounding environment rises. A shift towards shorter wavelengths, known as a blue shift, is observed in the emission maxima. Choosing a right buffer to work with antimicrobial peptides is important and HEPES buffer was chosen to work with four antimicrobial peptides namely cecropin B, melittin, aspidasept and three tryptophan modifications of NK-2 (I2W, F14W, G25W). In this study, sample quenching with different concentration of potassium iodide method were used to determine the degree of oligomerisation or the amount of oligomer formation. Additionally, SDS-PAGE method was also used to reveal the presence of oligomers.

Membrane binding of protein or peptides can induce conformational changes that affect the local environment tryptophan residues. These changes can lead to alterations in its fluorescence properties and in this study, blue shift effects were seen among all samples of AMPs. The Stern-Volmer constant (K_{sv}) values were calculated from quenching experiments for both fresh and stored samples. This study further showed that the K_{sv} value of most of the stored samples exhibited slightly a greater value compared to that of the fresh samples, suggesting that the stored samples experienced aggregation over the duration of the storage period, which potentially influencing the quenching efficiency.

Contents

1. Introduction	3
2. Theoretical Background	5
2.1 Tryptophan fluorescence	5
2.1.1 Stokes Shift.....	8
2.1.2 Solvent and Environmental Effects	9
2.1.3 Quenching of Fluorescence	9
2.1.4 Stern-Volmer Plots	10
2.2 Antimicrobial protein and peptides (AMPs)	11
2.3 Oligomerisation	15
3. Material and Methods	16
3.1 Material	16
3.1.1 Chemicals	16
3.1.2 Equipment and Software.....	17
3.2 Methods	17
3.2.1 Measurement of Fluorescence Emission Spectra and Fluorescence Quenching with Potassium Iodide	17
3.2.2 Denaturation of Lysozyme	19
3.2.3 Serial Dilution.....	19
3.2.4 Data Processing of Emission Spectra	19
3.2.5 Tricine SDS-PAGE.....	19
4. Results	21
4.1 Tryptophan Fluorescence Measurements	21
4.1.1 Buffer Comparison	21
4.1.2 Self-Quenching	23
4.2 Antimicrobial Protein (Lysozyme) Measurements	25
4.3 Antimicrobial Peptides (cecropin B, melittin, aspidasept, and NK-2 derivatives like I2W, F14W and G25W) Measurements	29
5. Discussion	39
6. References	42

1. Introduction

The development of novel antibiotics is essential due to the emergence of antibiotic resistance as an important issue in the realm of public health. The demand for novel therapies has led to the advancement of antimicrobial peptides (AMPs), which hold promising potential for practical applications in several domains including medicine, food production, agriculture, aquaculture, etc. AMPs are components of the innate immune response found in organisms ranging from prokaryotes to humans. All multicellular organisms produce antimicrobial peptides which are a diverse class of naturally occurring molecules functioning as their first line of defense mechanism [1]. These proteins have a wide range of direct killing capabilities against bacteria, yeast, fungi, viruses, and even cancer cells. AMPs can also be referred to as "host defense peptides" in higher eukaryotic organisms, which emphasizes their additional immunomodulatory functions [1]. Peptides with fewer than 100 amino acid residues and an overall positive charge (typically +2 to +9) are known as AMPs [2]. Most antibacterial AMPs are cationic AMPs that target bacterial cell membranes and break down the lipid bilayer structure, making them the most thoroughly studied AMPs to date. Most of these AMPs possess both hydrophilic and hydrophobic regions, making them amphipathic in nature. These structures give AMPs the ability to bind to phospholipid groups and hydrophobic regions of lipid components [3].

Antimicrobial peptides (aspidasept, cecropin B, melittin, NK-2 derivatives like I2W, F14W and G25W) permeabilizes bacterial cell membranes and its action is accompanied by the formation of membrane-associated oligomers. Aspidasept (Pep19-2.5) is a synthesized antimicrobial peptide (AMP) comprising 20 amino acids. It's capability lies in its efficient action against sepsis disease, where it binds and neutralizes endotoxins known as lipopolysaccharides (LPS) in gram-negative bacteria and lipoproteins/peptides (LP) in gram-positive counterparts [4,5]. The cecropins are a family of antibacterial peptides that range in length from 35 to 39 amino acids and are found in a variety of insect species as well as in mammals [6]. Cecropin B is a natural cationic AMP produced by silkworms and is the most potent AMP among cecropin family against some of the bacteria, such as *Bacillus subtilis*, *Mircococcus luteus*, *Streptococcus fecalis* AD-4, and *Pseudomonas aeruginosa* [7]. The anticancer properties of cecropins have been proven in earlier studies [8] such as inhibiting the growth of breast cancer cells [9]. Melittin contains 26 amino acids α – helical peptide and this peptide is the predominant component of bee venom [10]. The fluorescence of melittin, which contains a single tryptophan

residue, was examined by the use of tryptophan fluorescence spectroscopy by observing its emission maximum [11]. Including both gram-positive and gram-negative bacteria, melittin and cecropin are effective against a variety of infectious agents [12]. In a study, melittin and cecropin were analyzed and it is concluded that they are also capable of inhibiting cell-associated production of HIV-1 by suppressing HIV-1 gene expression [13]. I2W, F14W and G25W are modification of NK-2, a promising candidate for the development of antimicrobial drugs.

Before working on with the AMPs, tryptophan (Trp) measurement was performed on lysozyme to serve as a useful model system for studying the properties and behavior of antimicrobial peptides. Lysozyme is a stable and highly basic protein with a well-characterized structure, and it also contains six Trp residues that are useful for monitoring changes in the protein structure or environment. Several studies have been performed to evaluate the use of lysozyme along with Trp fluorescence. A study was carried out to examine the interaction between lysozyme and phospholipid bilayers, focusing on its effects on protein conformation and oligomerization [14]. The study utilized the quenching of Trp fluorescence and acrylamide quenching techniques to measure these effects [14]. The results indicated that the quenching of Trp fluorescence was accompanied by a blue shift in the emission maximum, suggesting that the individual Trp residues are differently accessible to the quencher [14]. In recent research, the interaction of synthetic cecropin B with *P. aeruginosa* was studied also using Trp fluorescence measurements to elucidate the mechanism of membrane rupture [15]. In a study about the penetration of synthetic cecropin B into *P. aeruginosa*, an observation was made with the partial quenching of Trp fluorescence by acrylamide [15]. The findings indicated that the degree of quenching was significantly reduced when the peptide was combined with *P. aeruginosa*, validating the perpendicular manner of penetration [15]. Another study investigated the process of melittin folding into an amphipathic helix and its interaction with membranes using Trp fluorescence spectroscopy [16]. In this research, the technique of Trp fluorescence spectroscopy was employed to examine the changes in the structure and dynamics of melittin during its interaction with membranes [16]. The main idea of their study was to analyze the variations in Trp fluorescence intensity or wavelength that occur as a result of melittin-membrane interactions. [16].

The aim of this study was to analyze the oligomerisation of six antimicrobial peptides (cecropin B, melittin, aspidasept, NK-2 derivatives like I2W, F14W and G25W) in the presence and

absence of a quencher (potassium iodide) using tryptophan fluorescence. By studying the effect of a quencher on the oligomerization of antimicrobial peptides, researchers can gain insights into how the presence of a quencher influences the peptide's conformation, aggregation, or membrane interactions. Exploring the oligomerisation of AMPs may help in the modification and development of AMPs.

2. Theoretical Background

2.1 Tryptophan fluorescence

Fluorescence is a process in which any substance (fluorophore) absorbs a photon of light at a specific wavelength and then re-emits or excites one or more electron within the substance at a higher energy state and resulting in a longer wavelength. This excited state is often referred as the single excited state. The Jablonski diagram (Fig.1) shows the processes that take place between light absorption and emission.

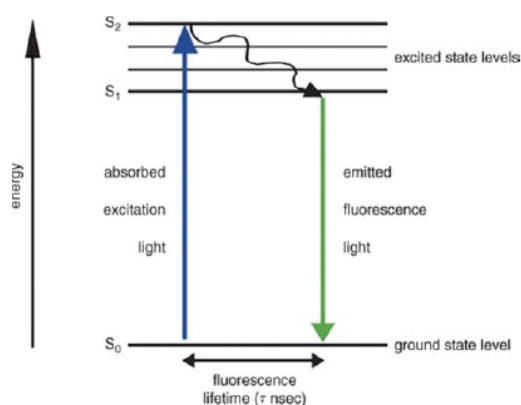


Figure 1: Jablonski diagram of Stokes shift phenomena of fluorescent compound with blue photon excitation and green photon emission [17].

On exposure to light of a specific wavelength, the electrons that are in the energetically lowest state S_0 can absorb a photon and move to a higher energy level known as the initial excited single state S_1 . The light's energy, which is dependent on its wavelength, must match the energy difference between S_0 and S_1 . The electron returns to S_0 while emitting a photon after releasing some of the energy as heat through a procedure known as vibrational relaxation. Fluorescence originates from electronic transitions that occur within aromatic amino acids, such as tryptophan (Trp, W), when electrons, which were initially displaced by incoming radiation, return from excited states within the protein structure to their original ground states.

Fluorescence can occur from both aromatic and non-aromatic molecules, although aromatic molecules are more commonly associated with fluorescence due to their ability to absorb and emit light in the visible or UV range. Aromatic molecules, such as those containing a benzene ring, have a characteristic conjugated p-electron system that allows them to absorb light at specific wavelengths. This absorption results in the excitation of the molecule to a higher energy state, followed by the emission of light at a longer wavelength, which is the fluorescence emission. However, fluorescence can also occur from non-aromatic molecules, such as fluorescent dyes or probes that have been designed specifically for this purpose. These molecules often contain a conjugated system of double bonds or other chemical groups that allow them to absorb and emit light. In addition, some non-aromatic molecules, such as certain proteins or enzymes, can exhibit fluorescence due to the presence of specific amino acids or cofactors that are capable of absorbing and emitting light [18].

The structure of a fluorophore typically consists of a conjugated system of double bonds, which allows for the absorption and emission of light. The conjugated system provides a series of energy levels within the molecule, enabling the absorption of photons and subsequent release of energy in the form of fluorescence. The structure of fluorophores plays a critical role in their ability to absorb and emit light. The key structural features that contribute to their optical properties are such as conjugated system, aromatic rings, functional groups, substituent and side chains, and solvent effects. Fluorophores may be broadly categorized into two main classes, namely intrinsic and extrinsic. Intrinsic fluorophores are naturally existing in nature. Meanwhile, extrinsic fluorophores are introduced into the sample in order to generate fluorescence in the absence of such, or to modify the spectrum characteristics of the material [18].

Tryptophan (Fig.2) is an example of an intrinsic fluorophore, meaning it is naturally present in certain biomolecules and exhibits fluorescence without the need for external labeling or modifications. It is an essential amino acid commonly found in proteins and is one of the 20 standard amino acids that make up the building blocks of proteins. The fluorescence of tryptophan arises from its unique structural and electronic properties. Tryptophan contains an indole ring, which consists of a benzene ring fused with a five-membered nitrogen-containing ring. The indole ring is responsible for the intrinsic fluorescence of tryptophan. When tryptophan is exposed to ultraviolet (UV) light with a wavelength around 280 nm, it absorbs the photons and undergoes an excitation process. The absorbed energy promotes an electron

within the indole ring to a higher energy level. Tryptophan has a strong absorption peak around 280 nm due to the presence of the indole chromophore. Following excitation, tryptophan rapidly relaxes back to its ground state through various relaxation pathways. One of the primary relaxation pathways is the emission of fluorescence. Tryptophan emits light at longer wavelengths, typically in the range of 320-350 nm, resulting in a blue fluorescence. The exact emission wavelength depends on the specific microenvironment of the tryptophan residue within the protein [18].



Figure 2: Structure of L-Tryptophan [19].

The fluorescence properties of tryptophan can be influenced by factors such as the surrounding environment, including pH, temperature, solvent polarity, and interactions with neighboring amino acids or ligands. These factors can alter the microenvironment around the tryptophan residue, affecting its fluorescence intensity and emission wavelength. Tryptophan fluorescence has been widely utilized in biochemical and biophysical studies. It serves as a sensitive probe for protein structure, dynamics, and conformational changes. By monitoring the fluorescence properties of tryptophan residues in proteins, researchers can gain insights into protein folding, ligand binding, protein-protein interactions, and enzymatic activity. It is important to note that while tryptophan is an intrinsic fluorophore, not all protein containing tryptophan residues exhibit strong fluorescence. The fluorescence intensity of tryptophan can be influenced by factors such as solvent exposure, quenching by nearby amino acid residues, or protein conformation. However, in proteins where tryptophan is properly exposed to the solvent and not strongly quenched, it can serve as a reliable and sensitive fluorescence probe.

Tryptophan appears to be particularly sensitive to quenching by a variety of substances, including iodide, acrylamide, and nearby disulfide groups [20]. Because of this sensitivity to quenchers, quenching measurements can be used to determine how accessible tryptophan residues are in proteins [21]. Tryptophan fluorescence quenching by iodide refers to the

reduction in fluorescence intensity emitted by the amino acid tryptophan in the presence of iodide ions.

2.1.1 Stokes Shift

When light interacts with a sample, the Stokes shift occurs, which is a spectral shift toward lower energy between the incident light and the dispersed or emitted light. The Stokes shift in fluorescence spectroscopy is the difference between the spectral location of the first absorption band's maximum and the highest fluorescence emission (Fig.3). In other words, it is the difference between the energy absorbed by the molecule and the energy released by the molecule.

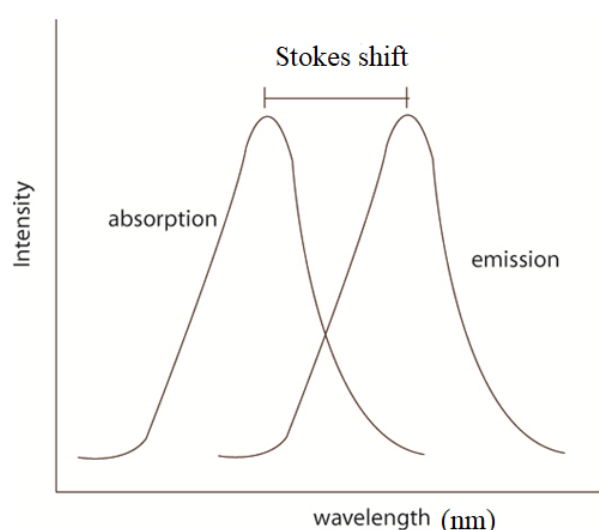


Figure 3: Stokes shift [22].

There is a term to describe changes in the wavelength of light and it is called red shift and blue shift. When a protein or peptides experience a conformational change that impacts the fluorophore's environment, the maximum emission wavelength of the fluorophore might be altered, either towards higher or lower wavelengths. If the emission wavelength is longer than the excitation wavelength, then the Stokes shift is a red shift. If the emission wavelength is shorter than the excitation wavelength, then it is a blue shift. In fluorescence, the red shift can be influenced by solvent relaxation.

2.1.2 Solvent and Environmental Effects

The properties of a fluorophore can be influenced by the surrounding solvent environment. Polar solvents can cause shifts in the absorption and emission spectra of the fluorophore. This phenomenon, known as solvatochromism, arises from interactions between the solvent and the fluorophore, altering the energy levels and electronic transitions. Solvent effects should be taken into consideration when designing fluorophores for specific applications [18].

2.1.3 Quenching of Fluorescence

Fluorescence quenching refers to the reduction or suppression of the fluorescence intensity emitted by a fluorescent molecule or chromophore. It occurs when the excited state energy of the fluorophore is non-radiatively transferred to another molecule or is lost through alternative pathways, rather than being emitted as fluorescence. Fluorescence quenching can be categorized into two major classifications: static quenching and dynamic quenching. The phenomenon of static quenching is characterized by the creation of a non-fluorescent compound between the fluorophore and the quencher. On the other hand, dynamic quenching is attributed to the transfer of energy between the fluorophore and the quencher resulting from collisions. Collisional quenching is a broad term that covers both static and dynamic quenching processes, with a particular focus on the influence of molecule collisions in the process of fluorescence quenching [18].

Self-quenching, also known as self-fluorescence quenching or concentration quenching, occurs when a high concentration of fluorophores leads to the reduction of fluorescence intensity. In self-quenching, the proximity of fluorophores to each other at high concentrations can result in energy transfer or other interactions that deactivate the excited state and prevent fluorescence emission. Self-quenching is a form of static quenching, where the fluorophore molecules interact with each other rather than with an external quencher molecule. The proximity of fluorophores can lead to the formation of non-fluorescent aggregates or dimers, which effectively deactivate the excited-state fluorophores. These interactions can include energy transfer, collision-induced processes, or self-association of the fluorophores. The extent of self-quenching depends on factors such as the concentration of fluorophores. At low concentrations, the fluorophores are typically well-separated, and fluorescence emission is observed. However, as the concentration increases, the probability of interactions between fluorophores also increases, leading to self-quenching and reduced fluorescence intensity. Self-quenching can be

problematic in certain experimental or assay setups where high fluorophore concentrations are required. It can limit the accuracy and sensitivity of fluorescence-based measurements. To mitigate self-quenching effects, dilution of the fluorophore solution or using lower concentrations of fluorophores is often employed [18].

2.1.4 Stern-Volmer Plots

Stern-Volmer plots are commonly used in fluorescence spectroscopy to investigate the dynamic quenching of fluorescence by a quencher molecule. This plot provides valuable information about the quenching process and the nature of the interaction between the fluorophore (the molecule emitting fluorescence) and the quencher. The Stern-Volmer equation describes the relationship between the fluorescence intensity of a fluorophore in the absence (F_0) and presence (F) of a quencher:

$$F_0/F = 1 + K_{sv}[Q]$$

Where F_0/F is the fluorescence intensity ratio, K_{sv} is the Stern-Volmer quenching constant, and $[Q]$ is the concentration of the quencher [20]. By plotting F_0/F as a function of $[Q]$, a Stern-Volmer plot is obtained. This plot typically exhibits a linear relationship when the quenching process follows a dynamic quenching mechanism, assuming a single type of quencher and a homogeneous system. The slope of the Stern-Volmer plot provides important information about the quenching process. The slope is directly related to the Stern-Volmer quenching constant (K_{sv}) and can be used to determine the efficiency of the quenching process. A higher slope indicates a more effective quenching process and stronger interaction between the fluorophore and the quencher. The intercept of the Stern-Volmer plot at $[Q] = 0$ represents the fluorescence intensity ratio in the absence of quencher, which is equal to 1 [18].

The Stern-Volmer quenching constant (K_{sv}) can also provide insights into the quenching mechanism. If K_{sv} is independent of the quencher concentration, it suggests a static quenching mechanism, where the fluorophore and quencher form a non-fluorescent complex. On the other hand, if K_{sv} varies with quencher concentration, it indicates a dynamic quenching mechanism, where the quencher interacts with the excited state of the fluorophore, resulting in fluorescence quenching [18].

2.2 Antimicrobial protein and peptides (AMPs)

Lysozyme was first discovered in 1921 by Sir Alexander Fleming, the same scientist who discovered penicillin, is an antimicrobial protein that has been found to be highly effective against microorganisms, particularly gram-positive bacteria. Lysozyme hydrolyzes the β -1,4-linkages between N-acetyl-D-glucosamine and N-acetylmuramic acid residues in the peptidoglycan of bacterial cell walls [23]. It is also known as muramidase or N-acetylmuramic hydrolase [24]. The catalytic activity of lysozyme is affected by several variables, such as pH, temperature, and the presence of specific ions. Depending on the source of the enzyme, the ideal pH for lysozyme activity varies, but it typically falls between 5 and 7. At pH levels that range from slightly acidic to neutral, it shows greater activity. The activity of the enzyme can be impacted by temperature changes, with the ideal temperature range typically falling between 25 and 37 degrees Celsius.

Proteins often contain multiple tryptophan residues situated in various environments, and each of these residues may have varying degrees of accessibility to quenchers. Complex Stern-Volmer plots and spectrum changes might be anticipated due to the selective quenching of tryptophan residues, which is reliant upon their exposure or burial. Lysozyme quenching is one illustration. Six tryptophan residues make up this egg white protein, several of which are thought to be close to the action site. The difference between the unquenched and quenched emission spectra can be used to calculate the emission spectrum of the quenched residues [20].

Antimicrobial peptides (AMPs) are a diverse class of small proteins or peptides that play a crucial role in the innate immune response of various organisms [25], including humans, animals, plants, and microbes. They are a part of the host defense system and provide protection against a wide range of pathogens, including bacteria, viruses, fungi, and parasites. AMPs exhibit broad-spectrum antimicrobial activity, meaning they are effective against a wide range of microorganisms. They can directly kill or inhibit the growth of pathogens by targeting various structures and mechanisms essential for their survival.

Most of AMPs are cationic (positive charge) and they typically have size in the range of 10 to 50 amino acid residues. These peptides frequently have a distribution of hydrophobic residues and basic amino acids that line up in three dimensions on opposing faces to create distinctive structures that are hydrophobic, positively charged, and water soluble [26]. The membrane adsorption and conformational changes occur because of the electrostatic interactions between

the positively charged antimicrobial peptides (AMPs) and the negatively charged cell membranes [27] [28] [29]. With their hydrophobic sides anchored in the hydrophobic lipid core of the bilayer, peptides bind to the membrane surfaces of cells. These peptides are specimens with C-terminal neutral hydrophobicity at their N-terminal ends, where they are plentiful in basic amino acids with strong alkalinity. The antibacterial and hemolytic properties are respectively correlated with the hydrophobicity and number of cationic net charges shown by these peptides [30].

The protein under investigation in this work is lysozyme, an antibacterial agent. The antimicrobial peptides being examined are listed in **Tab.1**.

Table 1: Amino acid sequence of the antimicrobial peptides (Cecropin B, Melittin, Aspidasept, I2W, F14W, G25W) used in this study.

Antimicrobial Peptides		Amino acid sequence
Aspidasept		GCKKY RRFRW KFKGK FWF ^W G
Cecropin B		KWKVF KKIEK MGRNI RNGIV KAGPA IAVLG EAKAL
Melittin		GIGAV LKVL ^T TGLPA LISWI KRKRQ Q
NK-2 derivatives	I2W	KWLRG VCKKI MRTFL RRISK DIL ^T G KK
	F14W	KILRG VCKKI MRTWL RRISK DIL ^T G KK
	G25W	KILRG VCKKI MRTFL RRISK DIL ^T W KK

Aspidasept is a synthetic polypeptide known as Pep19-2.5 and it has been investigated for its mode of action against infections, including sepsis-induced organ damage [5]. Aspidasept is a polypeptide compound that shows highly effective anti-lipopolysaccharide activity by effectively attaching to lipopolysaccharide molecules. This binding interaction enables the neutralization of endotoxins and subsequently leads to the expression of anti-inflammatory properties [31]. Furthermore, due to the composition of AMPs comprising natural amino acids, these compounds undergo quick metabolism within the body, hence avoiding the production of any toxic byproducts. The peptide also mitigates the pro-inflammatory effects of endotoxin generated by antibiotics in vivo and collaborates with conventional antimicrobial agents to reduce inflammation resulting from bacterial infections [32]. This phenomenon is characterized by a disruption of the bacterial membranes, resulting in an increase of the therapeutic effect of conventional antibiotics. Hence, the use of this a compound when combined with antibiotics may potentially serve as an essential component in the treatment of sepsis and several other infectious ailments, therefore potentially saving lives [32]. The presence of three tryptophan residues in aspidasept (Trp, ^W) is shown in **Tab. 1**.

Cecropins are a class of cationic antimicrobial peptides that were initially discovered in insects [33]. The majority of cecropins have an amphipathic N-terminal region and a mostly hydrophobic C-terminal segment, which typically takes on a helix-hinge-helix conformation [34]. Cecropin B having the most potent antimicrobial activity within the cecropin family is identified as being the one with the greatest potency [7]. Cecropin B exhibits a wide range of antimicrobial activity, effectively targeting both Gram-positive and Gram-negative bacteria, in addition to some fungi. It has been shown to be effective against various pathogenic bacteria, such as *Escherichia coli*, *Staphylococcus aureus*, and *Pseudomonas aeruginosa* [35].

Melittin, the main component of honeybee venom, has diverse biological and pharmacological characteristics. The significant surface action on lipid membranes, antimicrobial, anti-inflammatory, and anti-cancer effects of this substance have been thoroughly studied [36]. Melittin exhibits an interaction with cellular membranes, leading to the induction of pore formation. Consequently, this disrupts the normal functioning of the membrane and initiates the process of cell lysis [37]. An extensive amount of study has been dedicated to investigating the influence of melittin on the control of apoptosis, as well as the many variables that trigger apoptosis in diverse cancer types such as breast, ovarian, prostate, and lung cancer [38]. In the past few years, melittin has also attracted significant interest due to its considerable anti-protozoan effects. There is an increasing number of research revealing that several protozoan parasites such as *Leishmania*, *Plasmodium*, *Trypanosoma*, and *Toxoplasma* exhibit sensitivity to melittin [39].

An innovative peptide antibiotic, designated as NK-2, has been developed which shows improved antimicrobial efficacy toward negatively charged bacterial membranes. The development is achieved by drawing inspiration from the effector protein found in human immune cells, namely NK-lysin. It has been studied that NK-2 is effective against several bacteria [40] and against malaria parasites *Plasmodium falciparum* [41]. This antimicrobial agent has the potential to enhance the effectiveness of common chemotherapy treatments and might be beneficial in eliminating any remaining tumor cells following the surgical removal of solid tumors. The implementation of such a technique would provide protection against bacterial infections that may arise in conjunction with surgical procedures [42]. F14W, I2W, and G25W are modification of NK-2, the core region of the bactericidal protein NK-lysin. These modifications show potential as candidates for the development of antimicrobial drugs, therefore it is needed to conduct an extensive study of this matter.

The majority of experiments conducted up to this point have mainly examined the interactions of cationic peptides with model membrane systems [2]. In Fig. 4, some of the structural models of the AMP's mechanism in bacteria's membranes are highlighted.

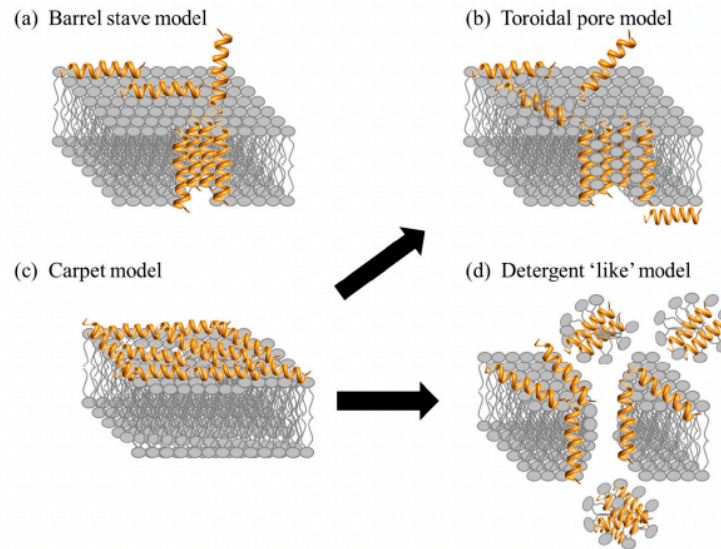


Figure 4: Mechanism of Action of AMPs in bacteria [43].

Electrostatic forces between AMPs's positive amino acid residues and the exposed negative charges on cell surfaces allow them to interact with microorganisms. Models of pore formation like the barrel-stave model and toroidal-pore model, moreover, models with no formation of pores like carpet model and detergent-like model have been put forth as potential explanations for how AMPs disrupt membranes [44]. Peptides produce trans membrane pores by being inserted directly into the lipid core of the target membrane, according to the "barrel-stave" model, which was the first mechanism proposed [45]. In this model, AMP binds to the membrane surface as a monomer before becoming an oligomer and forming pores [44]. The pore size may expand due to the recruitment of more monomers, resulting in the leakage of cytoplasm and eventual cell death. Example of AMP with the barrel-stave model is protegrin [44]. The "toroidal" model, in contrast to the "barrel-stave" model, involves the insertion of peptide molecules into the membrane to form a bundle, which causes the lipid monolayers to continuously bend through the pore [46]. As a result, the pore is formed by peptides interspersed between membrane lipids. Example of AMPs toroidal pore forming is melittin [44]. The "carpet" model postulates that AMPs cover the membrane surface and alter its architecture in a manner similar to detergent [47]. When the amount of AMPs on the membrane surface reaches a certain concentration, their interaction is initially fueled by electrical attraction, and the

membrane then separates, resulting in cell lysis [48]. Example of AMP with nonmembrane pore model is cecropin P1[44].

2.3 Oligomerisation

The process of joining or adding subunits to a base molecule to create new molecules is known as oligomerization. Protein oligomerisation can be defined as a process in which the monomeric units of protein are arranged into homo- or hetero- oligomers or to form higher structures, such as dimers, trimers, or larger oligomers. When stable proteins unfold, exposed interfaces for association interactions are created, which can lead to oligomerization [49]. Protein oligomers are usually made up of a limited number of monomers, ranging from two to ten. Protein oligomerization forms complex structures without increasing genome size and allows denaturation protection. AMP oligomers can cause membrane leakage by creating temporary pores, allowing critical nutrients and ions to escape.



Figure 5: Protein oligomers in antimicrobial activity [50].

As shown in Fig. 5, both amphiphilic peptides and proteins are capable to permeabilize cell membranes in oligomeric states and lead to cell death associated with antimicrobial activity. The number of molecules that come together depends on the sequence of the AMP, which determines whether a dimer or a higher order -oligomer is formed. The oligomerisation of proteins can be caused by a variety of factors, like ionic strength, pH, cofactors and nucleic acids [51]. The oligomerisation of antimicrobial peptides and proteins (AMPs) can be analyzed using tryptophan fluorescence, by monitoring its emission spectrum, changes in intensity, peak wavelength, and shifts.

3. Material and Methods

3.1 Material

3.1.1 Chemicals

Table 2: Used analytes.

Analyte	Molecular Weight [Da]	Article Number
DL-Tryptophan	204.23	1.08375.0025
Lysozym from chicken egg white	14,300	62971-50G-F

Table 3: Used antimicrobial peptides.

Antimicrobial Peptides	Molecular Weight [Da]	Article Number
Cecropin B	3,834.7	Providedby Prof. Jörg Andrä
Melittin	2,846,5	
Aspidasept	2,711.3	
I2W	3,275.2	
F14W	3,241.1	
G25W	3,331.2	

Table 4: Used solutions.

Solution	Molarity [M]
Guanidine HCl	8
Potassium iodide	5

Table 5: Used buffer solutions

Buffer	Molarity [M]	pH
Acetate	0.05	5.5
HEPES + NaCl	0.02 + 0.15	7.4
Phosphate	0.1	7.0

3.1.2 Equipment and Software

Table 6: Used equipment and software.

Device	Name	Manufacturer
Microplate reader	Infinite® 200 Pro	TECAN
96-well microtiter plates	Nunc™ F96 MicroWell™	Thermo Fischer Scientific
Data/Analysis software	Magellan™	TECAN

3.2 Methods

3.2.1 Measurement of Fluorescence Emission Spectra and Fluorescence Quenching with Potassium Iodide

The composition of the analyte-complex was carried out according to **Tab. 7**, where the buffer is prepared first (**Tab. 5**) then added with analyte. A 5 M potassium iodide solution was used as a quencher and were added to the final volume of 120 μL .

Different buffer/quencher volumes cause the quencher concentration to rise in each well, creating a quencher concentration gradient. As a reference, 120 μL buffer solution was pipetted into the wells. The mixing of the samples was done by setting up the TECAN software for 30 s shaking.

Table 7: Composition of the quencher complex.

Wells	Buffer [μL]	Analyte solution [μL]	KI solution [μL]	KI concentration [mol/L]
1	45	75	-	0
2	42.5	75	2.5	0.1
3	40	75	5	0.21
4	37.5	75	7.5	0.31
5	35	75	10	0.42
6	30	75	15	0.63
7	25	75	20	0.83
8	20	75	25	1.04
9	15	75	30	1.25
10	10	75	35	1.46
11	5	75	40	1.67
12	-	75	45	1.88

Samples were excited at 280 nm and emission spectra were subsequently recorded over time with range from 310 to 400 nm in 1 nm steps (**Tab. 8**). The 1 nm steps were used to measure the data because it provides higher spectral resolution than larger step sizes. From the obtained results the average value was calculated and blank subtracted. Quotient calculation I/I₀ against quencher concentration Q were performed with Microsoft Excel and ORIGIN.

Table 8: Used parameters for all carried out fluorescence emission spectra measurements.

Measurement Parameter	
Instrument	Infinite 200Pro
Instrument Serial Number	1208002678
Plate	
Plate Description	[NUN96fb] - Thermo Fisher Scientific - Nunclon 96 Flat Back
Plate with Cover	No
Barcode	No
Plate Shaking	30 s
Fluorescence Intensity Scan	
Scan Mode	Emission Scan
Emission Wavelength From	310 nm
Emission Wavelength To	410 nm
Emission Step Size	1 nm
Emission Number of Measurements	91
Excitation Wavelength	280 nm
Reading Mode	Top
Lag Time	0 μs
Integration Time	20 μs
Number of Reads	25
Settle Time	0 ms
Gain	Manual
Gain Value	100
Z-Position	Manual
Temperature	
Mode	On
Temperature	25 °C

3.2.2 Denaturation of Lysozyme

A lysozyme sample was prepared to measure the Ksv plot of denatured lysozyme, as directed in Experiment 10 (Georgie Institute of Technology, 2020). In deviation to the protocol, a solution of guanidine hydrochloride with a concentration of 8 M was used for denaturation, instead of a solution with a concentration of 6 M.

In this study, lysozyme that had been dissolved in acetate buffer was mixed in 8 M guanidine hydrochloride (GdnHCl) and subsequently adjusted to the desirable concentration, which was set at 0.1 mM. The lysozyme in GdnHCl was incubated at 55°C for at least 1 h.

3.2.3 Serial Dilution

Serial dilution was performed for each sample in 1.5 ml Eppendorf tubes and then was transferred on the 96-well plate. Samples were excited at 280 nm and emission wavelengths were recorded in the range 310–400 nm. Each mean value was formed from the measured data and plotted against wavelength. Then the curve was smoothed, and the blank was subtracted.

3.2.4 Data Processing of Emission Spectra

Fluorescence data were recorded and exported using TECAN's Magellan to excel. Data processing was done with Origin 2023b and Excel. To obtain the raw spectra, the mean value of the spectrum for each data were calculated in Excel. For smoothing of the curves, the method Savitzky-Golay, using 20 points of window was used in Origin.

3.2.5 Tricine SDS-PAGE

The experimental procedure involves the preparation of a tricine SDS-PAGE (**Tab. 9 – Tab. 13**). Two gels are poured and allowed to solidify. Subsequently, the gels are introduced into the reaction chamber, wherein running buffer solutions are employed to fill the chamber. To assure appropriate sample preparation, the concentration of each sample was chosen to be around 5 µg. The sample and sample buffer are mixed in the same amount and thereafter subjected to a temperature of 95°C for a duration of 5 minutes. A volume of 20 µL from each sample was carefully transferred into the designated gel pockets using a pipette. Subsequently, a constant electrical current with a magnitude of 40 mA is supplied for an estimated duration of 2.5 h. The time mentioned corresponds to the total duration of 2 h, which is necessary for the sample buffer to migrate through the gel. Additionally, duration of 30 min is allocated to

optimize the utilization of the gel's capacity. The gels are fixed using glutaraldehyde as described in the attached recipe. Subsequently, the gels are subjected to 4 h staining using a Coomassie staining solution. The destaining process is carried out using a destaining solution, followed by a final washing step involving three cycles of 5 min each using demineralized water.

Table 9: Composition for tricine SDS-PAGE gel.

Component	Separation Gel	Stacking Gel
30% Acrylamid	5.33 mL	1.28 mL
3 M Tris; pH 8.45, 0.3% SDS	3.33 mL	2.5 mL
Glycerol	1 mL	-
100% TEMED	3.3 µL	7.5 µL
Aqua dem.	306 µL	6.11 µL
10% APS	33 µL	100 µL

Table 10: Composition for running buffer SDS-PAGE (10x).

Component	Amount
1 M Tris Base	60.57 g
1 M Tricine	89.60 g
1% SDS	5.00 g
Adjust pH to 8.3, fill up up with aqua demineralized to 500 mL, dilute to 1x before use	

Table 11: Composition for gel fixing solution SDS-PAGE.

Component	Amount
5 % Glutardialdehyd	100 mL

Table 12: Composition for Coomassie-staining solution SDS-PAGE.

Component	Amount
100% acetic acid	50 mL
Coomassie blue G.250	0.125 g
Fill up with aqua demineralized to 500 mL	

Table 13: Composition for destaining solution SDS-PAGE.

Component	Amount
20% Ethanol	50 mL

4. Results

4.1 Tryptophan Fluorescence Measurements

4.1.1 Buffer Comparison

The literature provides extensive information on buffers used for fluorescence measurements of tryptophan (Trp). Phosphate or HEPES buffers are often used. Stern-Volmer plots were plotted for the analysis to determine which buffer is best for Trp fluorescence measurements and whether the choice of buffer affects the measurement. The Trp concentrations used for the experiment were 0.05 mM, 0.1 mM, and 0.2 mM. Trp fluorescence measurements were first conducted, followed by quenching with potassium iodide at the mentioned Trp concentrations.

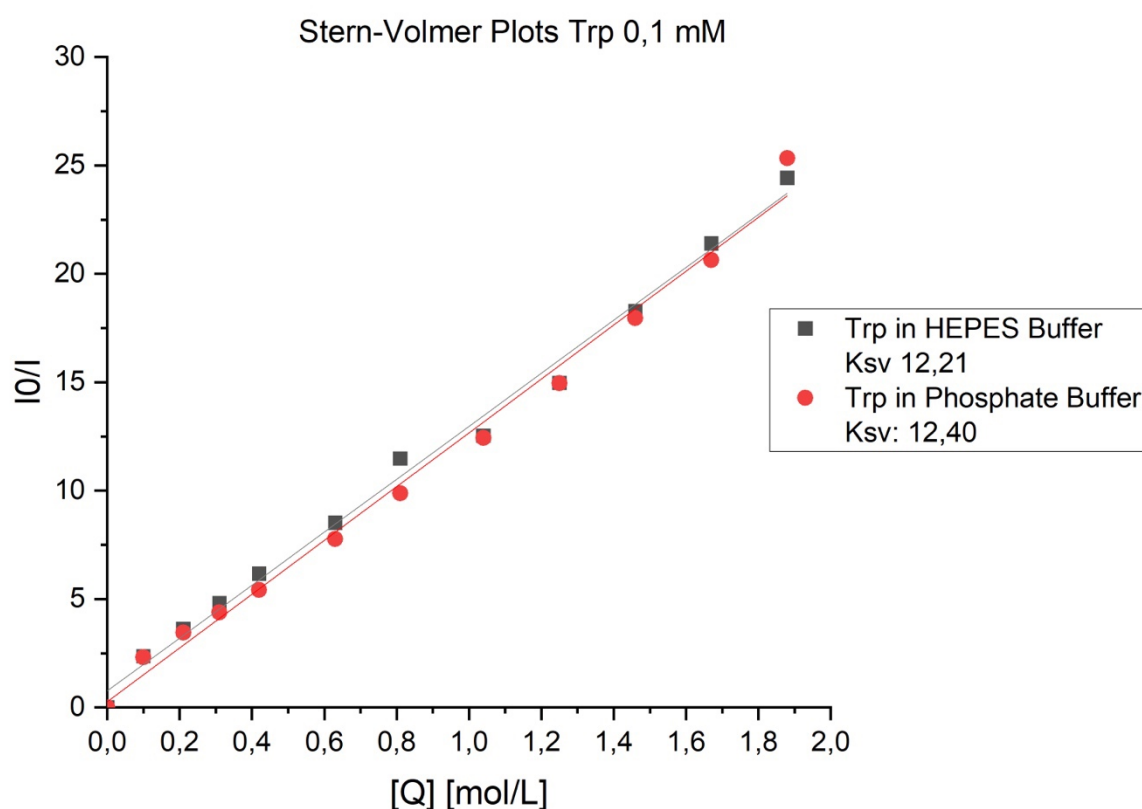


Figure 6: Stern-Volmer plots of 0.1 mM Trp solved in HEPES - and phosphate buffer.

0.1 mM of Trp solved in different buffers (HEPES and phosphate) and quenched with potassium iodide with increasing quencher concentrations. Each plot was created employing the mean value obtained from two independent experiments.

The experiment was conducted two times to rule out measurement errors. In Fig. 6, the average value of Ksv Trp 0.1 mM performed with phosphate buffer is slightly better in comparison with

HEPES buffer, given that the literature value of K_{sv} in tryptophan on iodide quenching is 12.8 M^{-1} [52]. Both buffer solutions are suitable for Trp measurement because they do not deviate much from the literature value. Nevertheless, phosphate buffer was chosen for further measurements with Trp.

Table 14: K_{sv} values of the measured Stern-Volmer plots of Trp in HEPES and phosphate buffer. n = number of experiments.

Buffer	c (Trp) [mmol/L]	K_{sv} [L/mol]	n
HEPES	0.05	9.5	1
		9.38	2
	0.1	12.74	1
		11.67	2
	0.2	15.86	1
		17.87	2
Phosphate	0.05	10.5	1
		8.22	2
	0.1	12.23	1
		12.6	2
	0.2	15.35	1
		14.75	2

4.1.2 Self-Quenching

A measurement limitation caused by high tryptophan (Trp) concentrations should be investigated for method development. As a result, the fluorescence spectrum of a series of Trp dilutions with a starting concentration of 100 mM was determined.

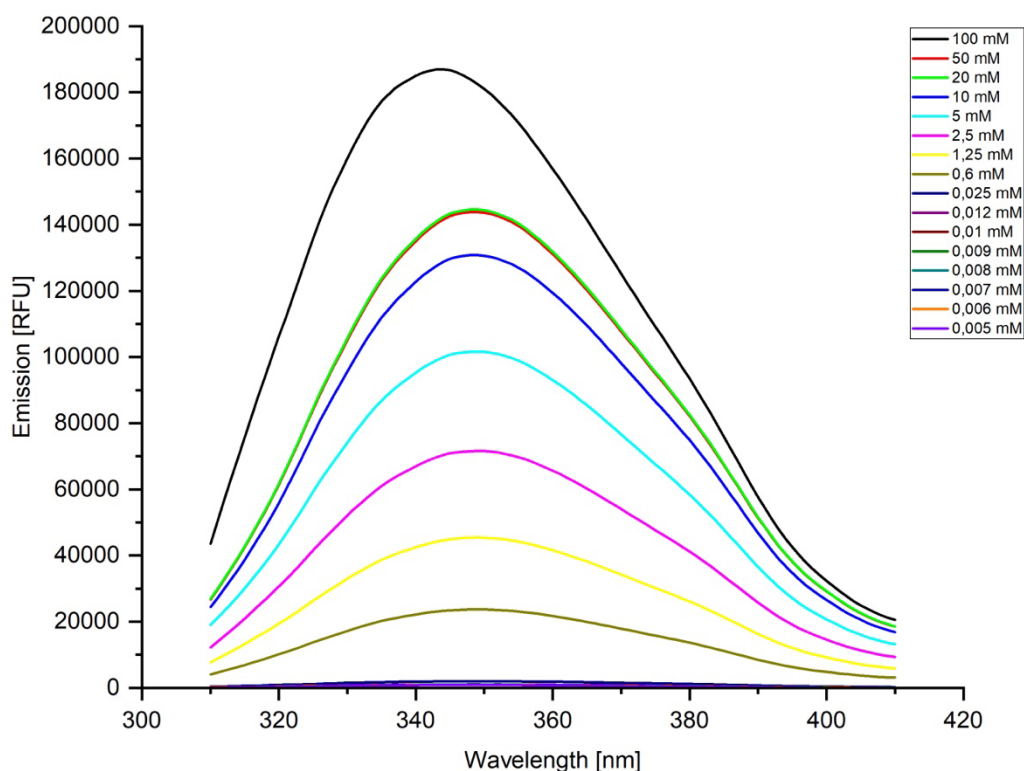


Figure 7: Emission spectra of serial dilution of Trp with a start concentration of 100 mM.

Serial dilution of Trp from 100 mM to 0.005 mM Trp was diluted in 0.1 M phosphate buffer with pH=7.0. After excitation at 280 nm, the fluorescence emission spectra were recorded. The graph represents the average results obtained from three independent experiments.

The spectra of the dilution series in Fig. 7 show a limitation of fluorescence from a tryptophan (Trp) concentration of 10 mM upwards, resulting in smaller fluorescence gains for doubling in concentration from 20 mM to 50 mM and a very high fluorescence intensity by 100 mM. The concentration from 0.6 mM to 10 mM resulting a gradual increase of fluorescence intensity as the concentration doubled. At lower concentrations, such as 0.025 mM downwards, the signals are weakening and barely visible on this graph.

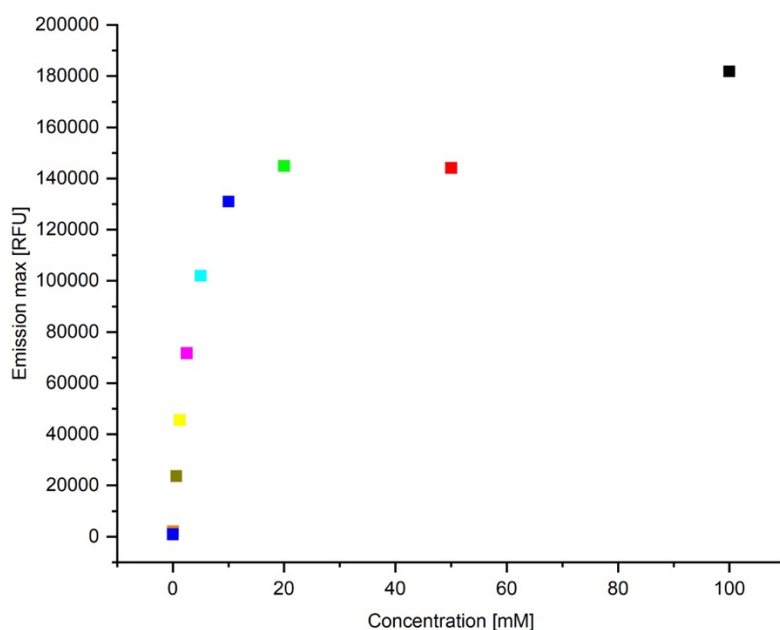


Figure 8: Emission maximum at 343 nm of measured Trp with concentration of 100 mM and at 350 nm of Trp concentration from 0.005 to 50 mM. The fluorescence maximum of Trp is at 350 nm.

A saturation by concentration between 20 mM and 50 mM was suspected to be the underlying cause of those observations. This saturation is caused by dependent self-quenching, in which the presence of nearby excited fluorophores causes the formation of excimers, non-fluorescent excited-state complexes. Fig. 8 also shows that increasing the concentration resulted in a slightly decreased fluorescence intensity, although at the highest concentration of Trp, at 100 mM, shows a significant rise that can also be affected due to the high concentration of Trp, allowing it to exhibit a higher emission maximum again.

Self-quenching shows, that it is crucial to keep the sample's tryptophan concentration under 10 mM when using tryptophan fluorescence spectroscopy because doing otherwise can result in significant measurement errors.

4.2 Antimicrobial Protein (Lysozyme) Measurements

Following the measurement of free tryptophan's fluorescence, we next investigated the fluorescence characteristics of tryptophan (Trp) embedded in a larger molecule to analyze the antimicrobial peptides. A well-studied protein, lysozyme, was chosen for the measurements because lysozyme has a high content of Trp residues (six Trp residues, three of them on the surface and three buried inside). A series of dilution of lysozyme were carried out in acetate buffer, and the fluorescence at each concentration was determined.

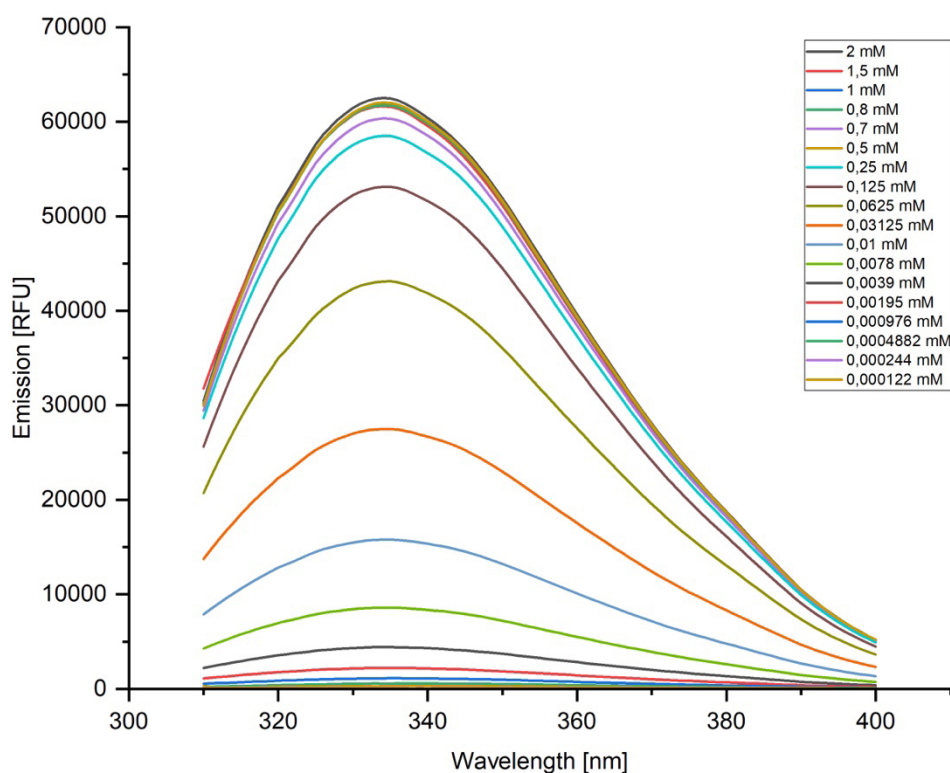


Figure 9: Emission spectra of native lysozyme at different concentrations starting from 2 mM. Serial dilution of lysozyme from 2 mM to 0.000122 mM was diluted in 0.05 M acetate buffer with pH= 5.5. After excitation at 280 nm, the fluorescence emission spectra were recorded. Emission maximum is at 334 nm.

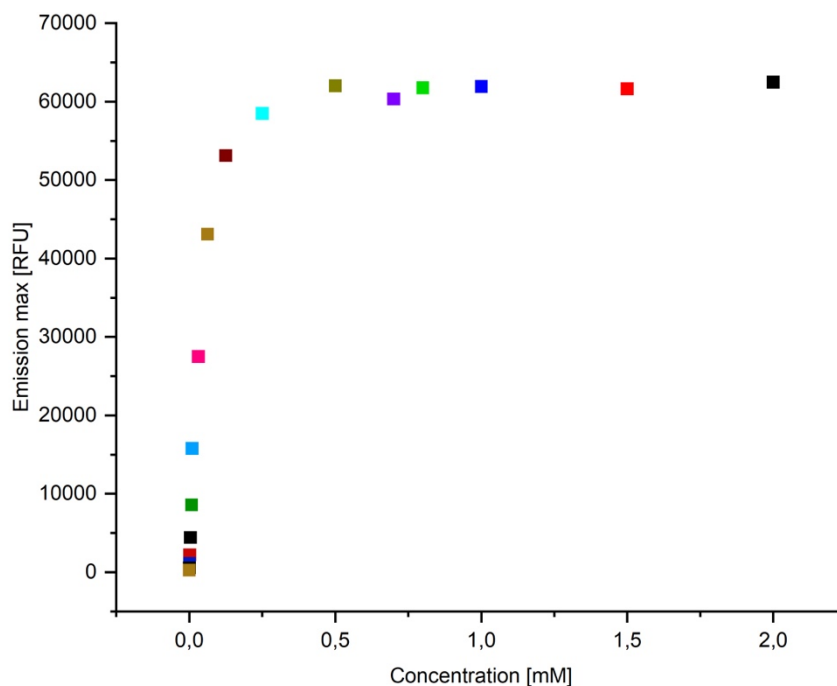


Figure 10: Emission maximum at 334 nm of measured lysozyme at different concentrations, starting from 0.000122 mM to 2 mM.

Fig. 9 and Fig. 10 illustrate how this dilution series, along with Trp measurement, improved self-quenching. When lysozyme is present at a concentration of 0.25 mM, as seen in Fig. 9, the fluorescence intensity is around 59,000 RFU. In contrast to the Trp fluorescence measurement shown in Fig. 7, it can be observed that at a concentration of 0.6 mM, Trp has the fluorescence intensity of around 20,000 RFU. The presence of six tryptophan residues in lysozyme accounts for its six-fold greater intensity compared to Trp at same concentrations.

Given the emission spectra of the native lysozyme dilution series, concentrations above 0.25 mM were assumed to cause the samples to self-quench because of the density and close proximity of molecules. With each concentration doubling, fluorescence intensity increases steadily at lower concentrations than it does at higher concentrations, where it only slightly changes. As it falls below the self-quenching threshold and is high enough to obtain a sufficient signal over the background noise, the concentration range of 0.0078 mM to 0.125 mM is considered suitable for further research.

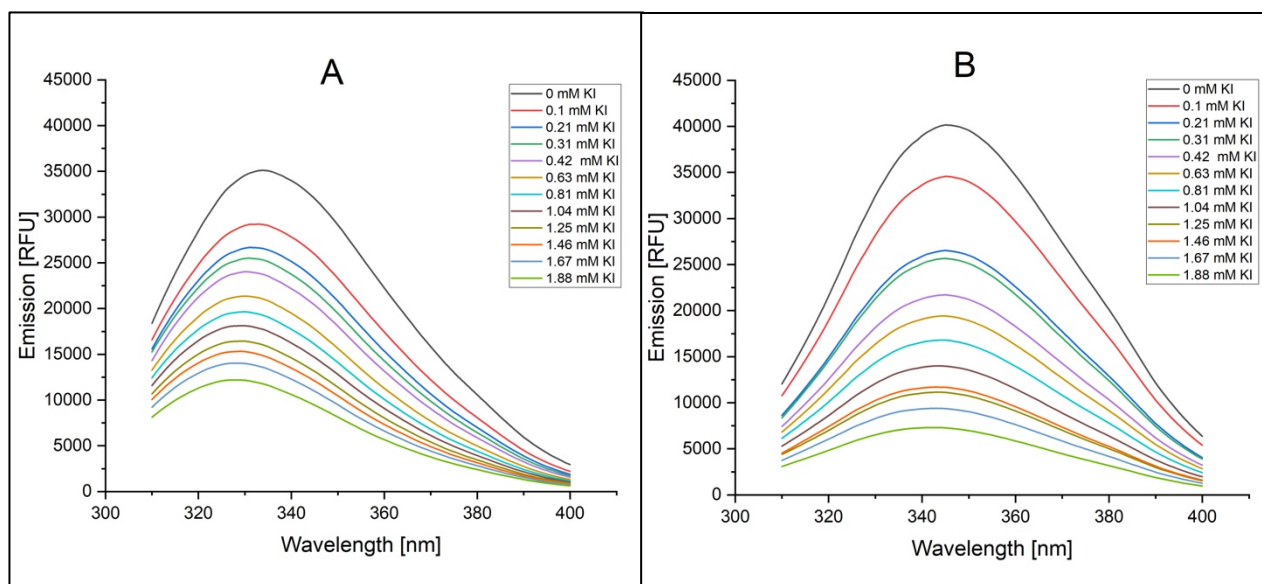


Figure 11: Emission spectra of lysozyme native (A) and denatured (B) in acetate buffer, quenched with potassium iodide. The concentration of the samples was 0.1 mM. The emission maxima are 331 nm for the native samples and 344 nm for the denatured. The apparent redshift is +13 nm and slightly increases with rising quencher concentration.

A concentration of 0.1 mM was then used for the fluorescence analysis of both native and denatured lysozyme. The denaturation of lysozyme was achieved by subjecting it to 8 M guanidine hydrochloride and then incubating it at 55°C for 1 h. A noticeable difference shift can be seen between the native- and denatured lysozyme emission spectra in Fig.11. The result of longer wavelength shifts in denatured lysozyme can be explained by the increased polarity of the environment in which Trp residues are exposed. This exposure makes Trp residues more accessible by the polar quencher and prevents them from being buried within the structure. This increased exposure to solvent molecules causes the emission to shift towards longer wavelengths, resulting in a redshift compared to the native state. In their native state, Trp residues are typically buried within the protein's structure, shielded from the surrounding solvent. The native conformation of lysozyme exhibits an emission maximum at around 331 nm, mainly attributed to the fluorescence of Trp residues within the protein. In the case of denatured lysozyme, the emission maximum is observed at around 344 nm, which can indicate changes in the environment's polarity or hydrophobicity due to the unfolding and exposure of previously buried Trp residues.

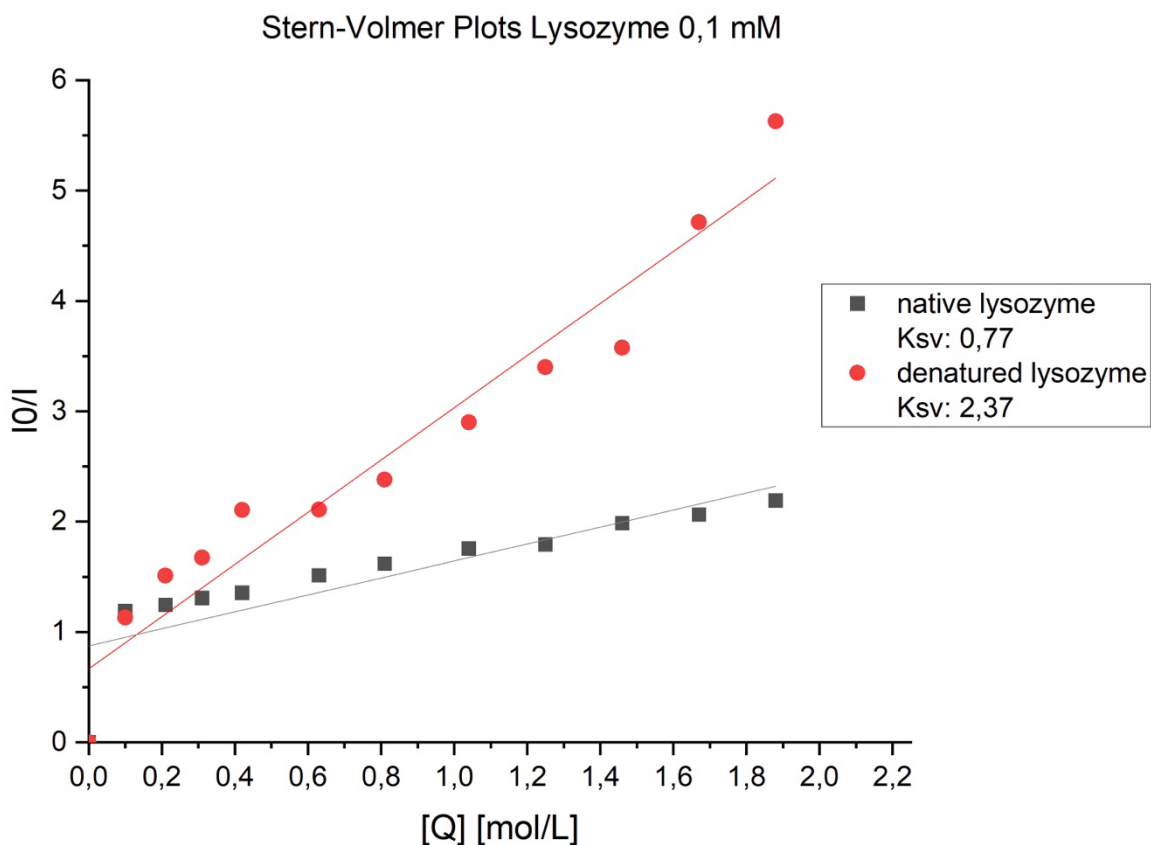


Figure 12: Stern-Volmer plots of native lysozyme solved in HEPES buffer and denatured lysozyme in acetate buffer using guanidine-hydrochloride as denaturation solution. The concentration of the samples was 0.1 mM with an increasing concentration of potassium iodide as a quencher. The values were measured at 331 nm for the native lysozyme and 344 nm for the denatured lysozyme.

Table 15: Results of K_{sv} determination of native and denatured lysozyme in acetate buffer (n=number of experiments).

Analyte	Buffer	c (Analyte) [mmol/L]	K_{sv} [L/mol]	n
Native lysozyme	Acetate	0.1	0.86	1
			0.77	2
			1.12	3
			1.01	4
Denatured lysozyme	Acetate	0.1	2.00	1
			2.07	2
			2.18	3
			2.37	4

By comparing the Stern-Volmer plots of both native and denatured forms of lysozyme in [Fig. 12](#) and the resulting K_{sv} in [Tab. 15](#), it was possible to prove the change of tertiary structure of lysozyme. The denatured version of the Stern-Volmer plot exhibits a significantly higher slope than the native form, providing evidence for the denaturation of lysozyme. This observation can be attributed to the increased accessibility of internal tryptophan residues to the quencher. Consequently, quenching efficiency is enhanced, resulting in a greater numerical value. [Tab. 15](#) shows, that the experiment was conducted four times to enhance reliability.

4.3 Antimicrobial Peptides (cecropin B, melittin, aspidasept, and NK-2 derivatives like I2W, F14W and G25W) Measurements

After fluorescence assays were conducted on the free tryptophan and the lysozyme (both native and denatured) samples, four antimicrobial peptides were studied. 0.02 M HEPES buffer with 0.15 M NaCl at a pH of 7.4 was used for experiments with the antimicrobial peptides (AMPs). HEPES buffer is commonly used for AMP experiments due to its excellent properties and biocompatibility. It is known for its pH stability, which is crucial for maintaining the integrity and activity of AMPs during fluorescence experiments. Adding NaCl to the HEPES buffer enhances the ionic potency of the AMPs, rendering the solvent-dependent properties of the AMPs analogous to in vivo environments.

A dilution series was then conducted to establish a range of concentrations for further measurements. The starting concentration of the dilution series was 0.05 mM, and this estimated concentration was derived from a dilution series of free Tryptophan. This concentration is still within a good range of concentration. In addition, due to the limited availability of peptides, a relatively low concentration was selected.

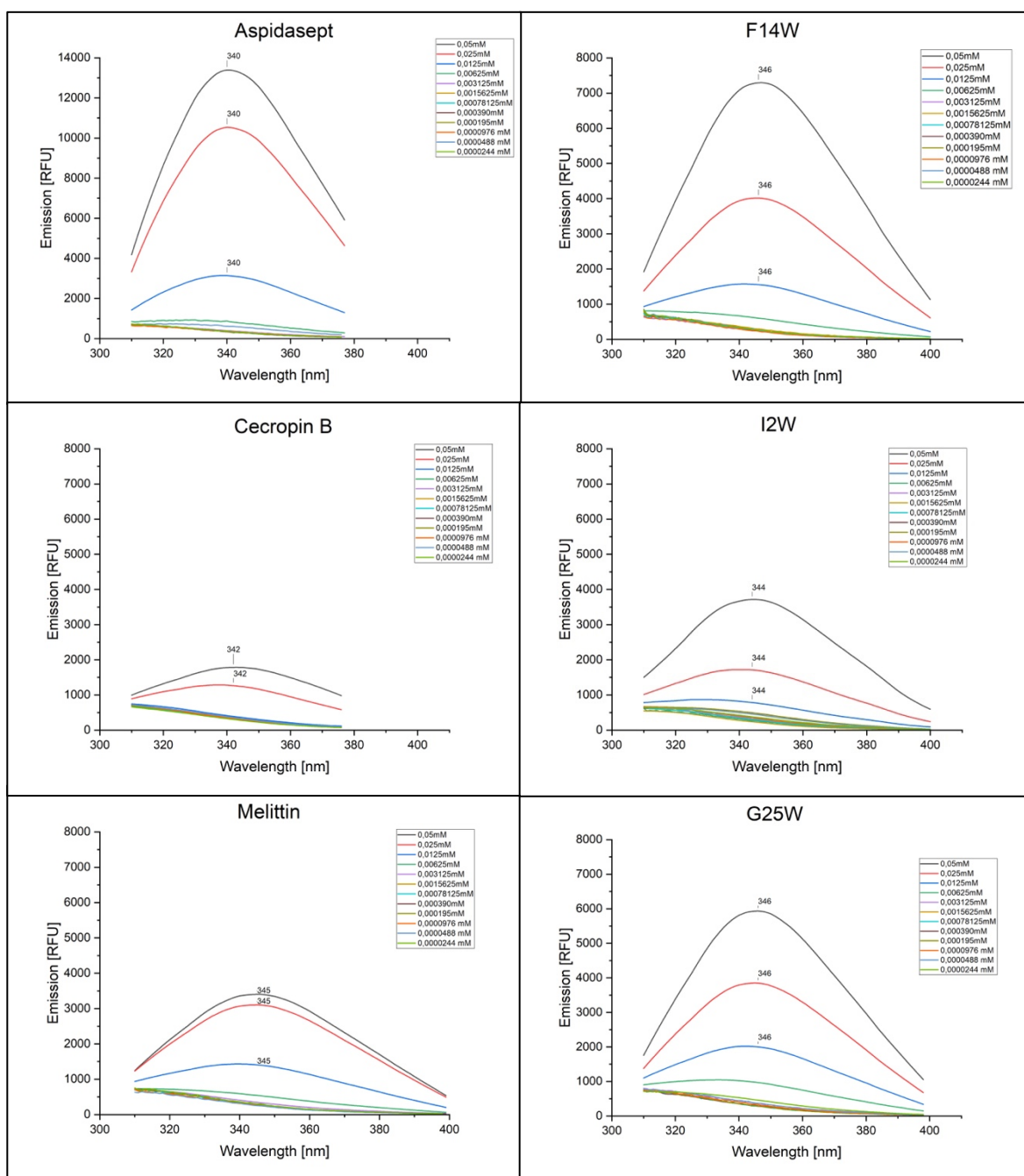


Figure 13: Emission spectra of a series of antimicrobial peptides (aspidasept, cecropin B, melittin, F14W, I2W, and G25W) with a starting concentration of 0.05 mM diluted in HEPES buffer.

Fluorescence emission spectra for six AMPs were recorded, after excitation at 280 nm. The wavelengths of the emission maxima (λ_{max}) for aspidasept 340 nm, cecropin B 342 nm, melittin 345 nm, F14W 346 nm, I2W 344 nm, and G25W 346 nm, are shown in Fig. 13.

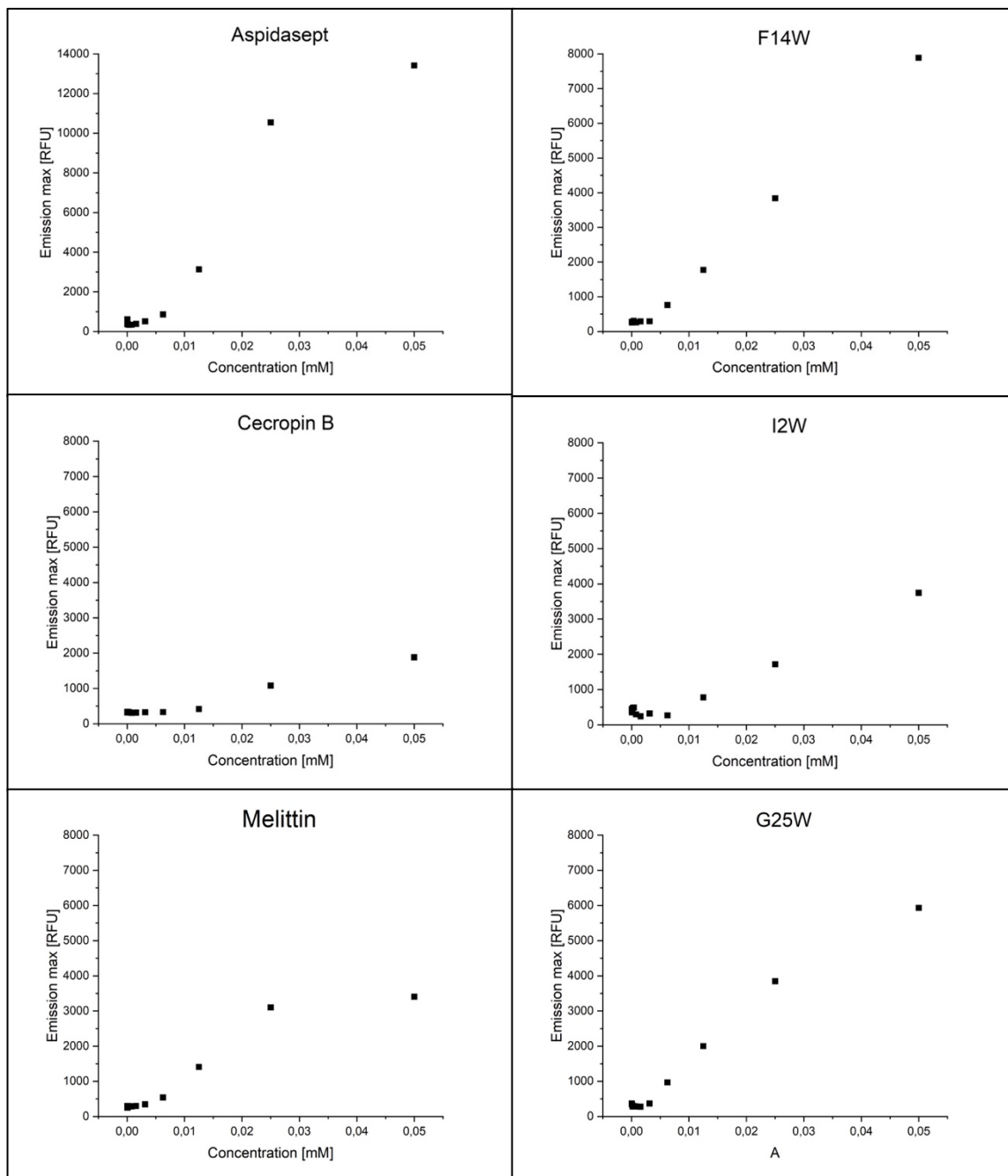


Figure 14: Emission maxima of series of antimicrobial peptides (aspidasept, cecropin B, melittin, F14W, I2W and G25W) with a starting concentration of 0.05 mM diluted in HEPES buffer. The wavelengths of the emission maxima (λ_{max}) for aspidasept 340 nm, cecropin B 342 nm, melittin 345 nm, F14W 346 nm, I2W 344 nm, and G25W 346 nm are shown.

Fig. 14 shows the absence of self-quenching at a given starting concentration for the dilution series of six AMPs. This suggests that at low concentrations, the fluorescence signal may be too weak to effectively quantify self-quenching. To determine the phenomenon of self-quenching at concentrations beyond 0.05 mM, greater concentrations were required. However, these concentrations weren't applied due to their costliness. The concentration of 0.05 mM was

selected with the consideration of the economical use of the peptides, and the reliability of the concentration was demonstrated to facilitate the study of the emission maxima of the fluorescence intensity exhibited by each of the samples depicted in Fig. 15.

The intensity of emission maximum of aspidasept at 13,418.70 RFU shows a relatively highest number compared with the other AMPs, as shown in Fig. 15. This condition is explained by the presence of three tryptophan residues in the amino acid sequence of aspidasept, that results in a threefold increase in its intensity compared to other antimicrobial peptides (AMPs), as expected. Meanwhile, cecropin B, melittin, and I2W shows relatively low emission maximum fluorescence intensity

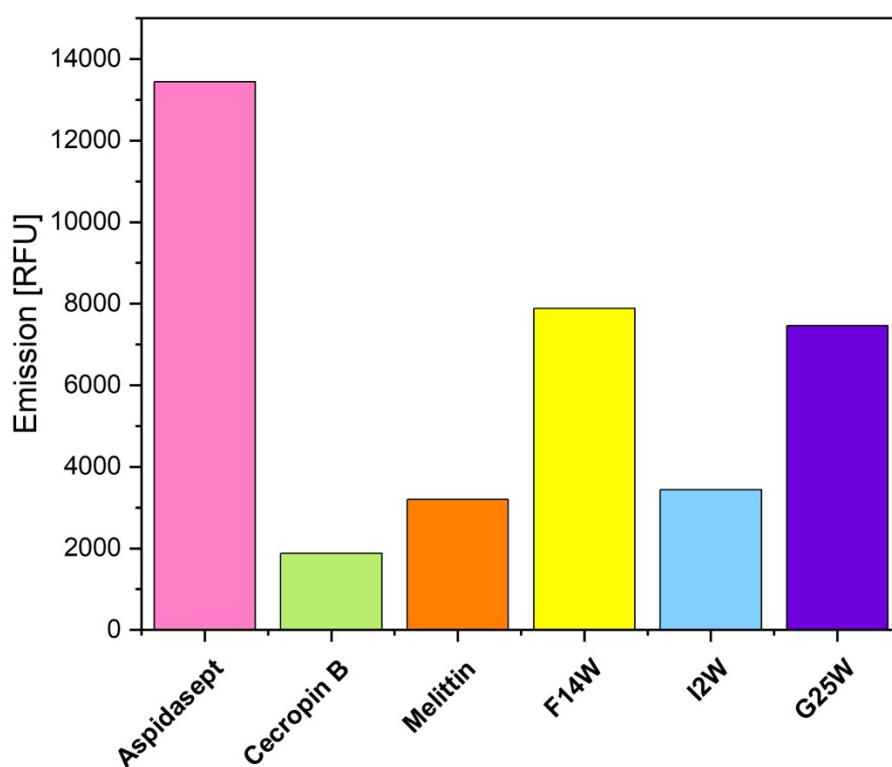


Figure 15: Emission maxima fluorescence intensity of dilution series of antimicrobial peptides (aspidasept, cecropin B, melittin, F14W, I2W and G25W) with starting concentration of 0.05 mM diluted in HEPES buffer. Number of Trp residues in aspidasept = 3, cecropin B = 1, melittin = 1, F14W = 1, I2W = 1, and G25W = 1.

The concentration of 0.05 mM was then utilized to generate the Stern-Volmer figure. The emission spectra of each sample were plotted against the wavelength to examine whether there were changes in emission maxima.

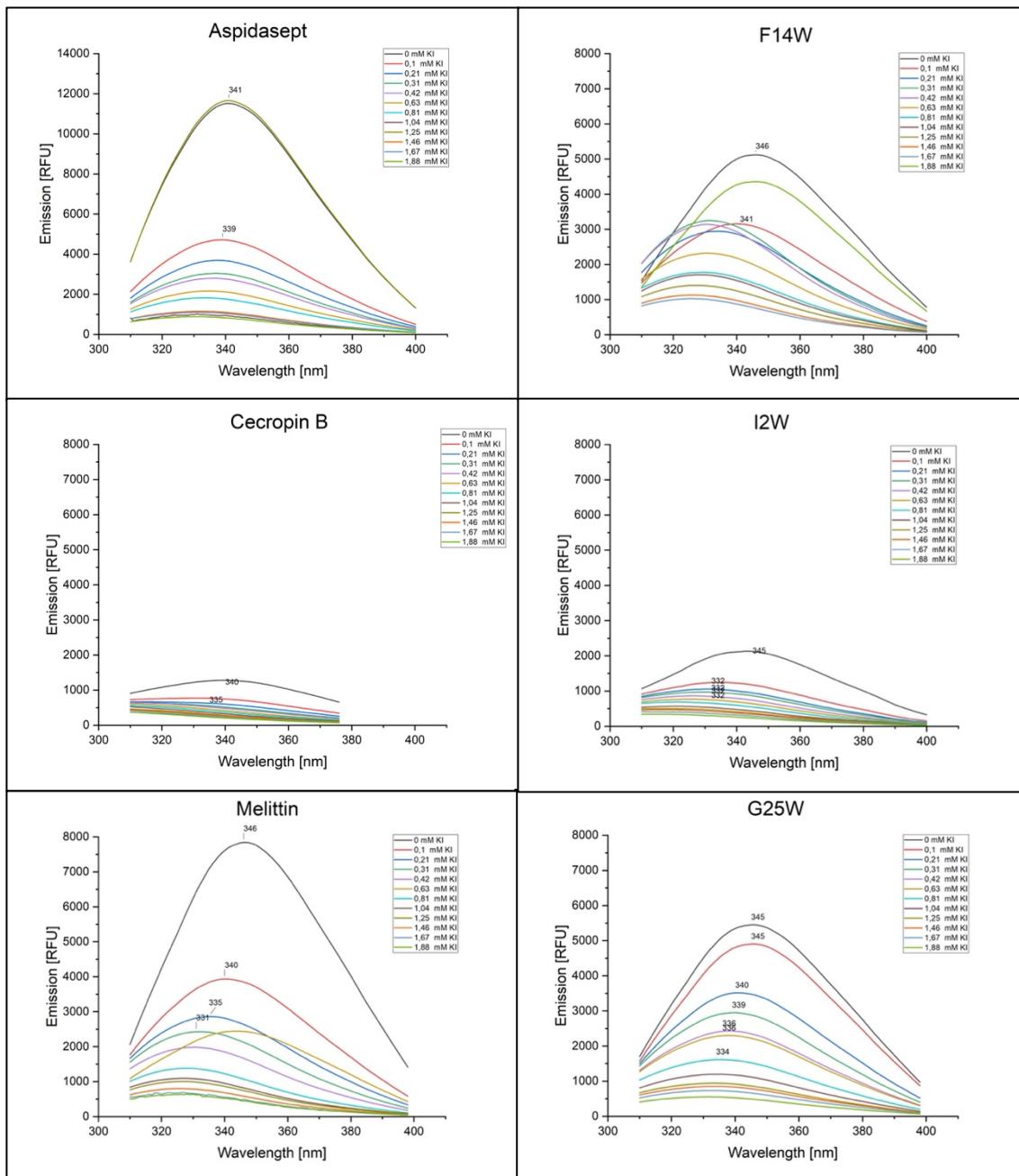


Figure 16: Emission spectra of a dilution series of antimicrobial samples (aspidasept, cecropin B, melittin, F14W, I2W and G25W) with starting concentration of 0.05 mM diluted in HEPES buffer, quenched with increasing concentration of potassium iodide.

Fluorescence emission spectra for six AMPs quenched with increasing potassium iodide concentration were recorded after excitation at 280 nm. The wavelengths of the emission maxima (λ_{max}) after quenching are for all AMPs gradually shifting to the shorter wavelengths (blue-shift), as shown in Fig. 16. The initial step of concentration for all AMPs, ranging from 0 mM to 0.1 mM KI, leads to a significant reduction in fluorescence intensity and blue-shift in

λ_{max} , suggesting a that the fluorophore is more “buried” inside the structure, and therefore less exposed to the solvent. The experimental findings indicate that when the quantity of the quencher increases, there is a consistent reduction in the intensity of fluorescence. This result suggests that fluorophores with higher accessibility display more sensitivity to changes in quencher concentration, resulting in a greater decrease in fluorescence intensity. Additional measurements were undertaken to compare the freshly obtained samples of antimicrobial peptides (AMPs) mentioned earlier with the stored samples of AMPs. This comparative analysis aimed to acquire a deeper understanding of the aggregation tendencies demonstrated by each sample. This was achieved by examining the emission spectra, quenched with potassium iodide, of both the freshly prepared and the stored samples. It is important to note that the aggregation phenomenon is intricate and influenced by various elements, such as the temperature of the storage and environmental conditions. The samples were maintained at a temperature of 5°C for two days before being subjected to the same measurement technique as the fresh samples.

According to the data presented in [Fig. 17](#) below, the emission maxima of stored aspidasept, cecropin B, I2W, and G25W exhibit no significant changes compared to their fresh samples. Otherwise, for melittin, F14W, and G25W, small alterations are seen in the fluorescence intensity and emission maximum. A minor alteration in the observed wavelength, compared to the data displayed in [Fig.17](#), indicates the existence of slight differences between fresh and stored samples. The potential aggregation of antimicrobial peptides during storage in a buffer solution is attributed to the presence of hydrophobic molecules, which may exhibit altered fluorescence characteristics compared to the fresh samples.

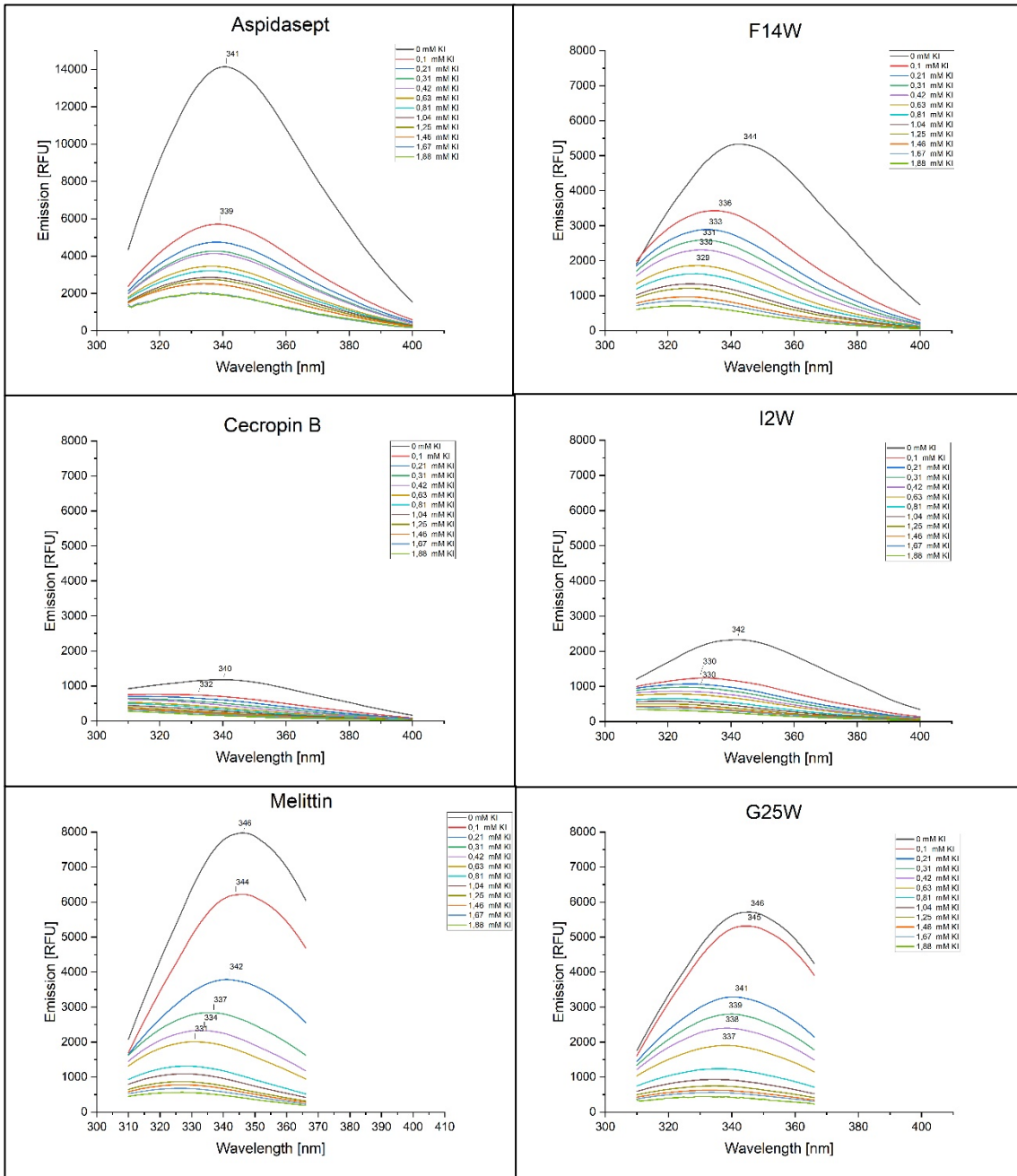


Figure 17: Emission spectra of a dilution series of stored antimicrobial samples (aspidasept, cecropin B, melittin, F14W, I2W and G25W) with starting concentration of 0.05 mM diluted in HEPES buffer, quenched with increasing concentration of potassium iodide.

Fig. 16 and Fig. 17 provide the basis for a closer look at the wavelength shifts, as seen in **Tab. 16**. There are no significant deviations in the maximum wavelength shift seen between the fresh and stored samples and this suggests that the storage condition of the samples does not have a substantial effect on the wavelength shift.

Table 16: λ_{\max} of AMPs (fresh and stored samples) without quencher and after quenching with potassium iodide 0.81 mM.

AMPs		Condition of AMPs	Quencher KI concentration [mM]	λ_{\max} [nm]	$\Delta\lambda_{\max}$ [nm]	
Aspidasept	Fresh		0	341	2	
			0.81	339		
	Stored		0	341	2	
			0.81	339		
Cecropin B	Fresh		0	340	10	
			0.81	330		
	Stored		0	340	8	
			0.81	332		
Melittin	Fresh		0	346	15	
			0.81	331		
	Stored		0	346	15	
			0.81	331		
NK-2 derivatives	F14W	Fresh	0	346	17	
			0.81	329		
		Stored		0	344	24
				0.81	320	
	I2W	Fresh		0	345	13
				0.81	332	
		Stored		0	342	12
				0.81	330	
	G25W	Fresh		0	345	11
				0.81	334	
		Stored		0	346	9
				0.81	337	

Nevertheless, due to the ongoing feature of a consistent blue-shift in the emission maxima for fresh and stored samples, it becomes necessary to adjust the observed wavelength for every concentration of the quencher to accurately account for the maximum point of each curve in the Stern-Volmer plot equation. The Stern-Volmer plots of each antimicrobial peptide (AMP) were displayed in Fig. 18 below, given numerically in a tabular format to ease comparison.

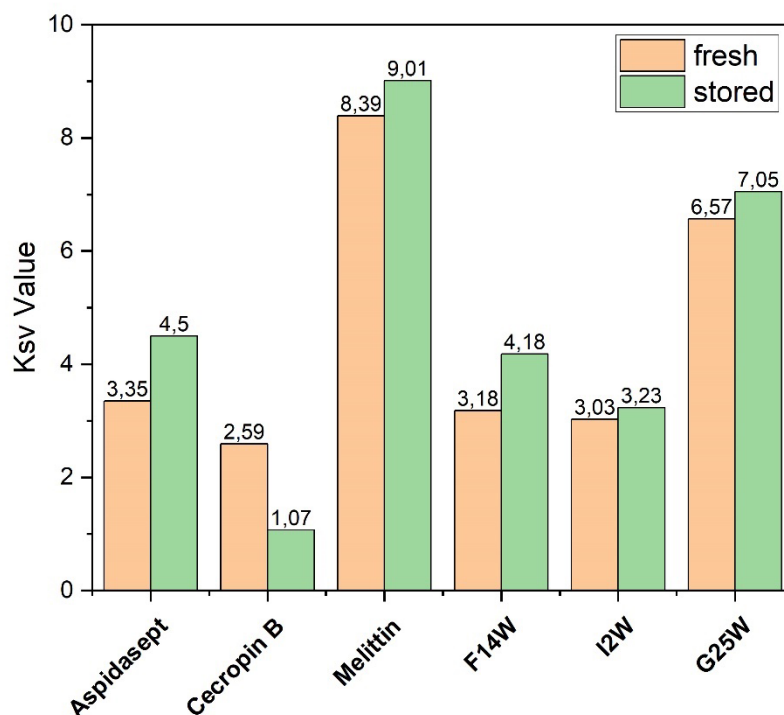


Figure 18: The Ksv values of antimicrobial peptide samples (aspidasept, cecropin B, melittin, F14W, I2W, and G25W) were determined for fresh and stored samples.

According to the data given in Fig. 18, it can be observed that the Ksv value of the stored samples is slightly higher than most of the fresh samples for all antimicrobial peptides studied. This observation can suggest an enhanced tendency of the peptides to go through aggregation or oligomerization throughout storage. The aggregation process can result in the proximity of fluorophores to quenching molecules, hence increasing the efficacy of quenching, and resulting in a higher number of Ksv.

Given the absence of significant variations in the wavelength shift and Ksv value, the stored samples of antimicrobial peptides were subsequently employed in the next step. The samples underwent analysis using SDS-PAGE, a combination of an analytical approach that provides further evidence and strengthen the earlier experiments regarding the oligomeric state.

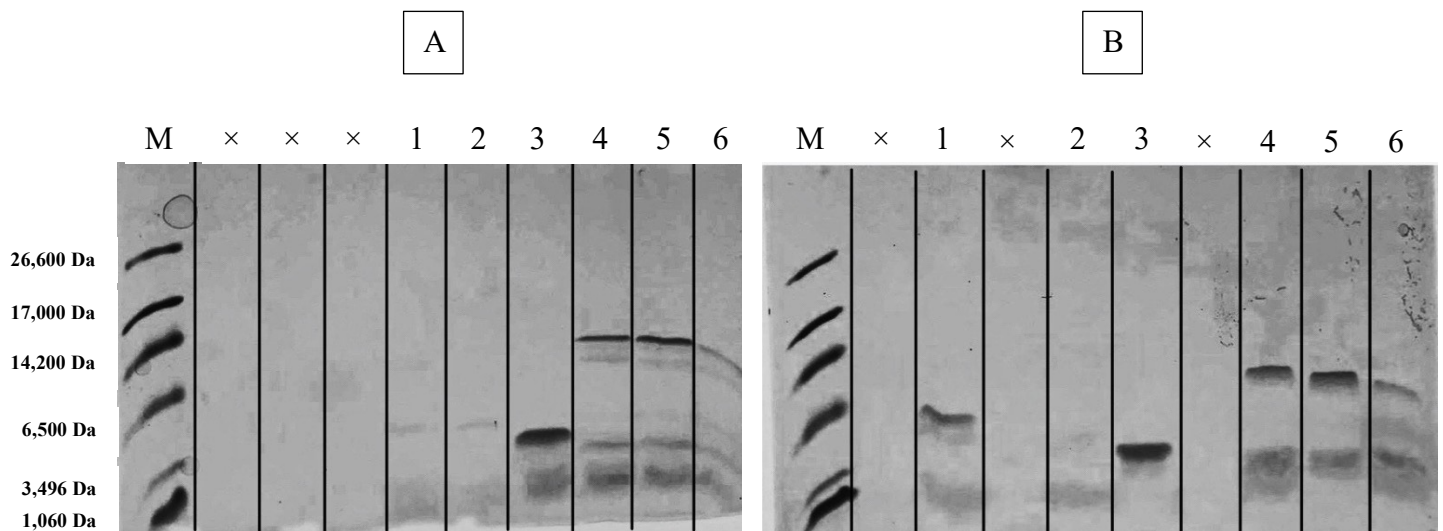


Figure 19: Antimicrobial peptides for SDS-PAGE analysis in unreduced gel (A) and reduced gel (B).

5 μ L marker and 20 μ L samples were pipetted onto the gel after incubation at 95°C for 5 min.

M=marker, x=SDS sample buffer (“empty gel” used as a gap), 1=aspidasept, 2=cecropin B, 3=melittin, 4=F14W, 5=I2W, and 6=G25W.

Two tricine SDS-PAGE gels were prepared and used for different analyses (unreduced gel analysis and reduced gel analysis). In reduced gel, the samples are treated with a reducing agent, such as dithiothreitol (DTT) and in unreduced gel, the samples are not treated with DTT and are directly pipetted onto the gel. A severe problem during the gel preparation process resulted in several air bubbles within certain gel sections. Thus, these areas were used as a gap containing no antimicrobial samples. Besides, the stacking gel used for the marker was not well formed, resulting in a gel band that revealed an unusually linear appearance.

5. Discussion

The tryptophan fluorescence measurement of a serial dilution of lysozyme starting from a concentration of 2 mM was conducted. The results showed a consistent emission maximum peak at 334 nm, which corresponds to the maximum emission wavelength of different tryptophan residues present in hen egg-white lysozyme [53]. Native- and denatured lysozyme with a lower concentration of 0.1 mM was then used for the quenching with potassium iodide (KI) in acetate buffer at pH 5.5, which showed an emission maximum of about 331 nm for native lysozyme (335 nm at pH 5.3 by Lehrer 1971 [52]). This observation can be considered an indication of the molecule's conformation. The detection of a blue shift in proteins, namely towards the shorter wavelength range of the emission maximum of tryptophan (Trp), indicates the presence of buried tryptophan residues within the hydrophobic core of the protein structure. These Trp residues cannot be quenched by Iodide, as Iodide primarily affects fluorophores located on the surface [54]. However, denatured lysozyme caused a red shift of the emission maximum to 344 nm similar to the maximum observed by Lehrer (1971). Following the denaturation process and next disruption of the molecules' three-dimensional structure, the tryptophan residues are released from the hydrophobic core, resulting in an emission maximum at a longer wavelength, commonly referred to as a red shift [52]. The luminescence of Trp residues inside a protein is seen to be significant, regardless of their location on the protein's surface or within its core. However, when doing a quenching experiment using an ionic quencher such the iodide ion, the quenching effect is observed exclusively on Trp residues that are localized on the protein's surface [55]. Therefore, the K_{sv} value of denatured lysozyme (2.37 M^{-1}) is higher than the native lysozyme (0.77 M^{-1}), meaning that the Trp residue is for the quencher more accessible, because it occurs in a hydrophilic environment and indicate that the Trp residue is exposed to that environment. The experimentally determined K_{sv} value of 2.37 M^{-1} corresponds to the literature value of 2.1 M^{-1} [52].

The emission peak of fresh sample of aspidasept in a 0.02 M HEPES buffer solution is observed at 341 nm prior to being quenched by potassium iodide. Following quenching, the emission peak is shifted gradually to shorter wavelengths with increasing KI concentration. Increasing accessibility Trp residues possess a higher sensitivity to changes in quencher concentration, resulting in a more significant decrease in fluorescence intensity [56]. There were no significant changes seen in the emission maximum of stored samples of aspidasept. The emission peak in the absence of a quencher occurs at a wavelength of 341 nm, and this peak is

seen to shift gradually from 339 nm to shorter wavelengths, similar to the behavior observed in the fresh samples. This phenomenon can be attributed to the greater degree of "burial" of the tryptophan residues inside the structure of aspidasept, leading to less exposure to the surrounding solvent. Consequently, a blue shift is observed. The fluorescence intensity of aspidasept is very high in comparison with other AMPs studied in this work, which can be attributed to the presence of three Trp residues within its amino acid sequence. The comparative analysis of the dependability of aspidasept in stored samples, as depicted in Fig. 17, indicates a better level of reliability in contrast to the fresh samples illustrated in Fig. 16. The reason for this discrepancy is that the emission spectra of the sample containing a concentration of 1.25 mM KI were not intended to align with the emission spectra of the sample without a quencher.

The emission maximum of F14W lies at 346 nm as shown in Fig. 13. The emission spectra of the stored sample of F14W in Fig. 17 show clear deviation from the fresh sample in Fig. 16 after quenching. For stored samples, there is a constant blue shift with increasing KI concentration. The observed result of a gradual blue-shift might be attributed to a comparable mechanism as revealed in the quenching processes of lysozyme and aspidasept. For G25W, there is an observed alteration in its fluorescence intensity, with a slight increase observed in stored samples. Both cecropin B and NK-derivative I2W show significantly reduced fluorescence intensity in both fresh and preserved samples compared with other AMPs. However, it is still noticeable that both samples likewise display a gradual blue shift as the concentration of KI increases.

The Stern-Volmer constant (K_{sv}) values for all antimicrobial peptides (AMPs) samples analysed in this study are presented in Fig. 18. It can be observed that the K_{sv} values for the stored samples are often greater than those of the fresh samples, except for cecropin B. It is interesting that the greatest K_{sv} value is found in melittin, even though aspidasept has three buried tryptophan residues and melittin only contains one. Based on the obtained data, it can be concluded that the K_{sv} value is independent of the Trp concentration. There is a potential correlation between the concentration of tryptophan residues and the Stern-Volmer constant. Therefore, further experimentation should be conducted to explore this connection. For further investigation, it is suggested that all AMP samples be subjected to denaturation, therefore

exposing the Trp residues to the solvent. This would enable a comparison of the K_{sv} value between the denatured and non-denatured samples of AMPs.

The aspidasept has a molecular weight of 2,711.3 Da and in both different gels shown in [Fig. 19](#), a faint band is detectable between 1,060 Da and 3,496 Da referring to a monomeric peptide. In unreduced and reduced gel, a distinct band was observed at around 6,500 Da or slightly higher. This band can be attributed to the double molecular weight of aspidasept, suggesting the presence of a dimerized structure and supporting the results of the fluorescence measurement of dimer formation. A similar observation was made for cecropin B, with a molecular weight of 3,834.7 Da. In the reduced gel, a faint band was observed, suggesting the presence of the monomeric form of cecropin B. Meanwhile, melittin, with a molecular weight of 2,846.5 Da, has a clear band on both gels at around 6,500 Da referring to its dimer structure. The NK-2 derivatives (F14W, I2W, and G25W) have similar band formation on the gel, clearly shown in [Fig. 19](#). The F14W, I2W, and G25W variants, with respective molecular weights of 3,241.1 Da, 3,275.2 Da, and 3,331.2 Da, exhibit a distinct band at around 3,496 Da in both gel samples, suggesting the presence of their monomeric structures. The visible appearance of a band between 14,200 Da and 17,000 Da in the unreduced gel indicates the aggregation of molecules into larger structures. The concentration of the samples under investigation was 5 µg. Based on the obtained data, it is suggested that increasing the concentration beyond 5 µg could improve the visibility of the gel band.

6. References

- [1] Ferenc-András, B., S. Zoltán-István, S. Erika, S. Pál, O. Csongor, and S. Edit(2019) Heterologous Expression and Purification of the Antimicrobial Peptide Buforin II. *Bulletin of Medical Sciences*. 92 (2), 119–125
(doi: 10.2478/orvtudert-2019-0010)
- [2] Giuliani, A., G. Pirri, and S. Nicoletto(2007) Antimicrobial peptides: an overview of a promising class of therapeutics. *Open Life Sciences*. 2 (1), 1–33
(doi: 10.2478/s11535-007-0010-5)
- [3] Bahar, A. and D. Ren(2013) Antimicrobial Peptides. *Pharmaceuticals*. 6 (12), 1543–1575(doi: 10.3390/ph6121543)
- [4] Heinbockel, L., S. Sánchez-Gómez, G. Martinez De Tejada, S. Dömming, J. Brandenburg, Y. Kaconis, et al.(2013) Preclinical Investigations Reveal the Broad-Spectrum Neutralizing Activity of Peptide Pep19-2.5 on Bacterial Pathogenicity Factors. *Antimicrobial Agents and Chemotherapy*. 57 (3), 1480–1487
(doi: 10.1128/AAC.02066-12)
- [5] Heinbockel, L., G. Weindl, W. Correa, J. Brandenburg, N. Reiling, K.-H. Wiesmüller, et al.(2021) Anti-Infective and Anti-Inflammatory Mode of Action of Peptide 19-2.5. *International Journal of Molecular Sciences*. 22 (3), 1465
(doi: 10.3390/ijms22031465)
- [6] Boman, H.G.(1995) Peptide Antibiotics and Their Role in Innate Immunity. *Annual Review of Immunology*. 13 (1), 61–92
(doi: 10.1146/annurev.iy.13.040195.000425)
- [7] Hultmark, D., A. Engstrom, H. Bennich, R. Kapur, and H.G. Boman(1982) Insect Immunity: Isolation and Structure of Cecropin D and Four Minor Antibacterial Components from Cecropia Pupae. *European Journal of Biochemistry*. 127 (1), 207–217 (doi: 10.1111/j.1432-1033.1982.tb06857.x)
- [8] Hui, L., K. Leung, and H.M. Chen(2002) The combined effects of antibacterial peptide cecropin A and anti-cancer agents on leukemia cells. *Anticancer Research*. 22 (5), 2811–2816
- [9] Zang, G., A. Thomas, and Z. Liu(2012) Preventing Breast Cancer Growth by Cationic Cecropin B. *Biological Systems: Open Access*. 02 (03)
(doi: 10.4172/2329-6577.1000112)
- [10] Habermann, E. and J. Jentsch(1967) Sequenzanalyse des Melittins aus den tryptischen und peptischen Spaltstücken. *Hoppe-Seyler's Zeitschrift Für Physiologische Chemie*. 348 (Jahresband), 37–50 (doi: 10.1515/bchm2.1967.348.1.37)

- [11] Tran, C.D. and G.S. Beddard(1985) Studies of the fluorescence from tryptophan in melittin. *European Biophysics Journal*. 13 (1) (doi: 10.1007/BF00266310)
- [12] Wade, D., D. Andreu, S.A. Mitchell, A.M.V. Silveira, A. Boman, H.G. Boman, et al.(2009) Antibacterial peptides designed as analogs or hybrids of cecropins and melittin. *International Journal of Peptide and Protein Research*. 40 (5), 429–436 (doi: 10.1111/j.1399-3011.1992.tb00321.x)
- [13] Brack-Werner, R., V. Erfle, N. Von Pechmann, M. Neumann, D. Winder, A. Kleinschmidt, et al.(1998) Antimicrobial peptides melittin and cecropin inhibit replication of human immunodeficiency virus 1 by suppressing viral gene expression. *Journal of General Virology*. 79 (4), 731–740 (doi: 10.1099/0022-1317-79-4-731)
- [14] Gorbenko, G.P., V.M. Ioffe, and P.K.J. Kinnunen(2007) Binding of Lysozyme to Phospholipid Bilayers: Evidence for Protein Aggregation upon Membrane Association. *Biophysical Journal*. 93 (1), 140–153 (doi: 10.1529/biophysj.106.102749)
- [15] Abou-Zied, O.K., A. Barbour, N.A. Al-Sharji, and K. Philip(2015) Elucidating the mechanism of peptide interaction with membranes using the intrinsic fluorescence of tryptophan: perpendicular penetration of cecropin B-like peptides into *Pseudomonas aeruginosa*. *RSC Advances*. 5 (19), 14214–14220 (doi: 10.1039/C4RA15246H)
- [16] Guha, S., J. Ghimire, E. Wu, and W.C. Wimley(2019) Mechanistic Landscape of Membrane-Permeabilizing Peptides. *Chemical Reviews*. 119 (9), 6040–6085 (doi: 10.1021/acs.chemrev.8b00520)
- [17] Llères, D., S. Swift, and A.I. Lamond(2007) Detecting Protein-Protein Interactions In Vivo with FRET using Multiphoton Fluorescence Lifetime Imaging Microscopy (FLIM). *Current Protocols in Cytometry*. 42 (1) (doi: 10.1002/0471142956.cy1210s42)
- [18] Ali, M.H. and B. Imperiali(2005) Protein oligomerization: How and why. *Bioorganic & Medicinal Chemistry*. 13 (17), 5013–5020(doi: 10.1016/j.bmc.2005.05.037)
- [19] Overcash, A., E. Griffing, S. Sukumara, and M. Overcash(2022) Environmental Sustainability Analysis of L-Tryptophan as a Consumer Product and Intermediate to Pharmaceutical Active Ingredients. *Frontiers in Sustainability*. 3 863914 (doi: 10.3389/frsus.2022.863914)
- [20] Lakowicz, J.R.(2010) Principles of fluorescence spectroscopy. Third edition, corrected at 4. printing *Springer, New York, NY*
- [21] Ladokhin, A.S.(2000) Fluorescence Spectroscopy in Peptide and Protein Analysis. in: R.A. Meyers (Ed.), *Encycl. Anal. Chem., John Wiley & Sons, Ltd, Chichester, UKp. a1611*(doi: 10.1002/9780470027318.a1611)
- [22] Skoog, D.A., F.J. Holler, and S.R. Crouch(2007) Principles of instrumental analysis. 6th ed *Thomson Brooks/Cole, Belmont, CA*

- [23] Shahmohammadi, A.(2018) Lysozyme separation from chicken egg white: a review. *European Food Research and Technology*. 244 (4), 577–593 (doi: 10.1007/s00217-017-2993-0)
- [24] Zhang, H., G. Fu, and D. Zhang(2014) Cloning, Characterization, and Production of a Novel Lysozyme by Different Expression Hosts. *Journal of Microbiology and Biotechnology*. 24 (10), 1405–1412 (doi: 10.4014/jmb.1404.04039)
- [25] Zhang, Q.-Y., Z.-B. Yan, Y.-M. Meng, X.-Y. Hong, G. Shao, J.-J. Ma, et al.(2021) Antimicrobial peptides: mechanism of action, activity and clinical potential. *Military Medical Research*. 8 (1), 48 (doi: 10.1186/s40779-021-00343-2)
- [26] Jenssen, H., P. Hamill, and R.E.W. Hancock(2006) Peptide Antimicrobial Agents. *Clinical Microbiology Reviews*. 19 (3), 491–511 (doi: 10.1128/CMR.00056-05)
- [27] Garreis, F., M. Gottschalt, T. Schlorf, R. Gläser, J. Harder, D. Worlitzsch, et al.(2011) Expression and Regulation of Antimicrobial Peptide Psoriasin (S100A7) at the Ocular Surface and in the Lacrimal Apparatus. *Investigative Ophthalmology & Visual Science*. 52 (7), 4914 (doi: 10.1167/iovs.10-6598)
- [28] Garreis, F., M. Gottschalt, and F.P. Paulsen(2010) Antimicrobial Peptides as a Major Part of the Innate Immune Defense at the Ocular Surface. in: H. Brewitt (Ed.), *Dev. Ophthalmol.*, S. Karger AG, pp. 16–22 (doi: 10.1159/000315016)
- [29] Sharma, P., S. Guha, P. Garg, and S. Roy(2018) Differential expression of antimicrobial peptides in corneal infection and regulation of antimicrobial peptides and reactive oxygen species by type III secretion system of *Pseudomonas aeruginosa*. *Pathogens and Disease*. 76 (1) (doi: 10.1093/femspd/fty001)
- [30] Lei, J., L. Sun, S. Huang, C. Zhu, P. Li, J. He, et al.(2019) The antimicrobial peptides and their potential clinical applications. *American Journal of Translational Research*. 11 (7), 3919–3931
- [31] Su, J., S. Wu, F. Zhou, and Z. Tong(2023) Research Progress of Macromolecules in the Prevention and Treatment of Sepsis. *International Journal of Molecular Sciences*. 24 (16), 13017 (doi: 10.3390/ijms241613017)
- [32] Heinbockel, L., G. Weindl, G. Martinez-de-Tejada, W. Correa, S. Sanchez-Gomez, S. Bárcena-Varela, et al.(2018) Inhibition of Lipopolysaccharide- and Lipoprotein-Induced Inflammation by Antitoxin Peptide Pep19-2.5. *Frontiers in Immunology*. 9 1704 (doi: 10.3389/fimmu.2018.01704)
- [33] Hoskin, D.W. and A. Ramamoorthy(2008) Studies on anticancer activities of antimicrobial peptides. *Biochimica et Biophysica Acta (BBA) - Biomembranes*. 1778 (2), 357–375 (doi: 10.1016/j.bbamem.2007.11.008)
- [34] Wang, J., K. Ma, M. Ruan, Y. Wang, Y. Li, Y.V. Fu, et al.(2018) A novel cecropin B-derived peptide with antibacterial and potential anti-inflammatory properties. *PeerJ*. 6 e5369 (doi: 10.7717/peerj.5369)

- [35] Elhag, O., D. Zhou, Q. Song, A.A. Soomro, M. Cai, L. Zheng, et al.(2017) Screening, Expression, Purification and Functional Characterization of Novel Antimicrobial Peptide Genes from *Hermetia illucens* (L.). *PLOS ONE*. 12 (1), e0169582 (doi: 10.1371/journal.pone.0169582)
- [36] Wang, A., Y. Zheng, W. Zhu, L. Yang, Y. Yang, and J. Peng(2022) Melittin-Based Nano-Delivery Systems for Cancer Therapy. *Biomolecules*. 12 (1), 118 (doi: 10.3390/biom12010118)
- [37] Memariani, H., M. Memariani, H. Moravvej, and M. Shahidi-Dadras(2020) Melittin: a venom-derived peptide with promising anti-viral properties. *European Journal of Clinical Microbiology & Infectious Diseases*. 39 (1), 5–17 (doi: 10.1007/s10096-019-03674-0)
- [38] Pandey, P., F. Khan, M.A. Khan, R. Kumar, and T.K. Upadhyay(2023) An Updated Review Summarizing the Anticancer Efficacy of Melittin from Bee Venom in Several Models of Human Cancers. *Nutrients*. 15 (14), 3111 (doi: 10.3390/nu15143111)
- [39] Memariani, H. and M. Memariani(2021) Melittin as a promising anti-protozoan peptide: current knowledge and future prospects. *AMB Express*. 11 (1), 69 (doi: 10.1186/s13568-021-01229-1)
- [40] Schröder-Borm, H., R. Willumeit, K. Brandenburg, and J. Andrä(2003) Molecular basis for membrane selectivity of NK-2, a potent peptide antibiotic derived from NK-lysin. *Biochimica et Biophysica Acta (BBA) - Biomembranes*. 1612 (2), 164–171 (doi: 10.1016/S0005-2736(03)00115-9)
- [41] Gelhaus, C., T. Jacobs, J. Andrä, and M. Leippe(2008) The Antimicrobial Peptide NK-2, the Core Region of Mammalian NK-Lysin, Kills Intraerythrocytic *Plasmodium falciparum*. *Antimicrobial Agents and Chemotherapy*. 52 (5), 1713–1720 (doi: 10.1128/AAC.01342-07)
- [42] Schröder-Borm, H., R. Bakalova, and J. Andrä(2005) The NK-lysin derived peptide NK-2 preferentially kills cancer cells with increased surface levels of negatively charged phosphatidylserine. *FEBS Letters*. 579 (27), 6128–6134 (doi: 10.1016/j.febslet.2005.09.084)
- [43] Kumar, P., J. Kizhakkedathu, and S. Straus(2018) Antimicrobial Peptides: Diversity, Mechanism of Action and Strategies to Improve the Activity and Biocompatibility In Vivo. *Biomolecules*. 8 (1), 4 (doi: 10.3390/biom8010004)
- [44] Luo, Y. and Y. Song(2021) Mechanism of Antimicrobial Peptides: Antimicrobial, Anti-Inflammatory and Antibiofilm Activities. *International Journal of Molecular Sciences*. 22 (21), 11401 (doi: 10.3390/ijms222111401)
- [45] Ehrenstein, G. and H. Lecar(1977) Electrically gated ionic channels in lipid bilayers. *Quarterly Reviews of Biophysics*. 10 (1), 1–34 (doi: 10.1017/S0033583500000123)

- [46] Yang, L., T.A. Harroun, T.M. Weiss, L. Ding, and H.W. Huang(2001) Barrel-Stave Model or Toroidal Model? A Case Study on Melittin Pores. *Biophysical Journal*. 81 (3), 1475–1485 (doi: 10.1016/S0006-3495(01)75802-X)
- [47] Rotem, S. and A. Mor(2009) Antimicrobial peptide mimics for improved therapeutic properties. *Biochimica et Biophysica Acta (BBA) - Biomembranes*. 1788 (8), 1582–1592 (doi: 10.1016/j.bbamem.2008.10.020)
- [48] Oren, Z. and Y. Shai(1998) Mode of action of linear amphipathic α -helical antimicrobial peptides. *Biopolymers*. 47 (6), 451–463(doi: 10.1002/(SICI)1097-0282(1998)47:6<451::AID-BIP4>3.0.CO;2-F)
- [49] Liu, S.(2015) A review on protein oligomerization process. *International Journal of Precision Engineering and Manufacturing*. 16 (13), 2731–2760(doi: 10.1007/s12541-015-0349-x)
- [50] Liu, C. and J. Luo(2023) Protein Oligomer Engineering: A New Frontier for Studying Protein Structure, Function, and Toxicity. *Angewandte Chemie International Edition*. 62 (23), e202216480 (doi: 10.1002/anie.202216480)
- [51] Kumari, N. and S. Yadav(2019) Modulation of protein oligomerization: An overview. *Progress in Biophysics and Molecular Biology*. 149 99–113 (doi: 10.1016/j.pbiomolbio.2019.03.003)
- [52] Lehrer, S.(1971) Solute perturbation of protein fluorescence. Quenching of the tryptophyl fluorescence of model compounds and of lysozyme by iodide ion. *Biochemistry*. 10 (17), 3254–3263 (doi: 10.1021/bi00793a015)
- [53] Nishimoto, E., S. Yamashita, N. Yamasaki, and T. Imoto(1999) Resolution and Characterization of Tryptophyl Fluorescence of Hen Egg-White Lysozyme by Quenching- and Time-Resolved Spectroscopy. *Bioscience, Biotechnology, and Biochemistry*. 63 (2), 329–336 (doi: 10.1271/bbb.63.329)
- [54] Möller, M. and A. Denicola(2002) Protein tryptophan accessibility studied by fluorescence quenching. *Biochemistry and Molecular Biology Education*. 30 (3), 175–178 (doi: 10.1002/bmb.2002.494030030035)
- [55] Lindon, J.C., G.E. Tranter, and D.W. Koppenaal, Eds.(2017) Encyclopedia of spectroscopy and spectrometry. Third edition *Elsevier/AP, Academic Press is an imprint of Elsevier, Amsterdam ; Boston*
- [56] Dos Santos Rodrigues, F.H., G.G. Delgado, T. Santana Da Costa, and L. Tasic(2023) Applications of fluorescence spectroscopy in protein conformational changes and intermolecular contacts. *BBA Advances*. 3 100091(doi: 10.1016/j.bbadv.2023.100091)